



Dedicate

This thesis is dedicated to:

My great parents, who never stop giving of themselves in countless ways,

My beloved uncle and aunts

To my dear sisters,

To all my family, the symbol of love and giving,

My friends who encourage and support me,

Lianeamel

Dedicate

This thesis is dedicated to:

Mom and Dad who always pic me up on time and encouraged me to go on

Every adventure, specially this one;

My great parents, who never stop giving of themselves in countless ways,

My beloved brother and sisters

My supportive husband ;

My dear friends

Kamari Fatima

Acknowledgment

In the Name of Allah, the Most Merciful, the Most Compassionate all praise be to Allah, the Lord of the worlds; and prayers and peace be upon Mohamed His servant and messenger.

First and foremost, we must acknowledge my limitless thanks to Allah, the Ever-Magnificent; the Ever-Thankful, for His helps and bless. I am totally sure that this work would have never become truth, without His guidance.

We would like to express our special appreciation and thanks to our advisor Dr. Lila Mouffok for encouraging our research and for allowing us to take a step forward. Your advice on both research as well as on our career have been invaluable.

We would like to thank the faculty and administration of institute of Aeronautics and Space Studies (IAES), for the wealth and quality of their teaching and making great efforts to ensure to their students an updated training

We would especially like to thank Mr Azemdroub for his support when we collected data for our thesis and helping us in many things, just, thank you.

A special thanks to our family. Words cannot express how grateful we are to our mothers and our fathers for all of the sacrifices that they've made on our behalf. Your prayer for us was what sustained us thus far, without forgetting to thank our brothers and sisters.

Finally, we would like express my gratitude to all the people who helped me by providing their valuable assistance and time

Abstract

In this work, a design of directive wideband, low profile, bowtie antenna operating in the C band is proposed. To achieve this purpose, we propose to use AMC reflectors.

The CST MWS software is used for designing and simulations. The obtained results show that the proposed antenna operates in the 4.08 - 6.4 GHz and show a quasi-stable realized gain in broadside direction with a maximum enhancement realized gain of 8.8 dBi compared to antenna without AMC.

Résumé

Dans ce travail, on propose de concevoir une antenne sous forme de papillon directive, large bande et à faible épaisseur fonctionnant dans la bande C. Pour atteindre cet objectif, on introduit des réflecteurs à Conducteurs Magnétiques Artificiels (AMC).

Le logiciel CST Microwave Studio est utilisé pour la conception et les simulations. Les résultats obtenus montrent que l'antenne proposée fonctionne dans la bande 4,08 - 6,4 GHz et présente dans la direction broadside un gain réalisé quasi stable et une amélioration maximale de 8,8 dBi par rapport à une antenne sans AMC.

ملخص

في هذا العمل، مقترح تصميم هوائي يربط معبأل وندمج، الغرض من هذا العمل هو تصميم هوائي لالهوائي المقترح مع كسطح عاكس للهوائي استخدام سطح AMC لتحسين كسب الهوائي و للحصول على نطاق واسع، بأصغر حجم ممكن تمت عملية التصميم و المحاكات باستخدام برنامج CST MWS 2017 النتائج المتحصل عليها توضح ان مكسب الهوائي تم تعزيزه واستقراره على طول عرض نطاق التشغيل.

Content

Acknowledgment.....	4
Abstract	5
Figures list	8
Abbreviations	10
Introduction	12
CHAPTER I	14
Chapter I: Satellite System For navigation and communication	15
I.1 introduction	15
I.2 Global Navigation Satellite Systems.....	15
I.2.1Current global navigation satellite system	16
I.2.2 GNSS signals	18
I.2.3 Measuring principle	19
I.3.Satellite Communication Systems.....	20
I.3.1 Satellite Communications Spectrum	21
I.3.2 Elements of Satellite Communications System.....	22
I.4 Various Types of Antenna with Respect to their Applications (antennas for space applications).....	27
I.4.1 Microstrip Patch Antenna:.....	27
I.4.2 spiral antenna	28
I.4.3 Helical antenna.....	29
I.4.4 Phased array antenna.....	29
I.4.5Mesh reflector:	30
I.4 Conclusion	31
CHAPTER II	32
Chapter II:EBG structure and state of the art on wideband antenna with Artificial Magnetic Conductor	33
II.1 Introduction.....	33
II.2 Background.....	33
II.3 EBG definition.....	34
II.4 Characterization of EBG structures	35
II.5 EBG applications in antenna engineering.....	38
II.5.1 Application for surface wave suppressions.....	38
II.5.2 Application for efficient low profile wire antenna designs.....	39

II.5.3 Reflection/transmission surfaces for high gain antennas.....	40
II.6 State of the art on wideband antennas with Artificial Magnetic Conductor.....	41
II.7 Conclusion:.....	48
Chapter III	49
ChapterIII:Wideband bow-tie antenna with an Artificial Magnetic Conductor (AMC).	50
III.1 Introduction	50
III.2 CST Microwave Studio Simulator	50
III.3 Bowtie Antenna.....	50
III.4 AMC reflector design.....	51
III.5 Bowtie antenna over artificial magnetic conductor.....	54
III.6 Parametric study.....	58
III.6.1Influence of the parameter L_{cps}	58
III.6.2 Influence of the parameter L_p	59
III.6.3 Influence of the parameter W_p	60
III.6.4Influence of the parameter W_{add}	61
III.6.5 Influence of number of vias.....	62
III.7 Optimized structure	63
III.8 Conclusion.....	65
Conclusion and perspectives	66

Figures list

Figure 1 Examples of everyday GNSS applications (1).....	16
Figure 2 Satellite communication(6).....	21
Figure 3 Signal processing elements in satellite communications	22
Figure 4 Element of satellite communication system.....	23
Figure 5 Repeater transponder. b Regenerative transponder.....	24
Figure 6 Shows a schematic block diagram of an earth station.....	26
Figure 7 example of patch antenna.....	28
Figure 8 representation of spiral antenna (11).....	28
Figure 9 helical antenna	29
Figure 10 Mesh reflector used in cubesat for Earth Science and Deep Space mission (16)	30
Figure 11 Periodic structure 1D, 2D, 3D (18)	34
Figure 12 Geometry of mushroom-like electromagnetic band gap (EBG) structure	35
Figure 13 LC model for the mushroom-like EBG structure ; (a) EBG parameter ,(b) model LC.....	36
Figure 14 Example of reflection phase.....	38
Figure 15 shows a comparison of patch antennas with and without EBG structures.....	39
Figure 16 EBG substrate for a low profile curl antenna design (from [24] C _ Wiley InterScience) ..	40
Figure 17 A high gain resonator antenna designs using an EBG structure	41
Figure 18 Geometry of Bowtie antenna and composite antenna (23)	42
Figure 19 Photograph of fractal AMC plane(23)	42
Figure 20 Unit cell of proposed AMC structure ,.....	43
Figure 21 The Bowtie antenna.(24).....	44
Figure 22 Element of the manufactured prototype ,(a) double bowtie antenna ,(b)AMC unit cells arrangement ,(c) Bowtie AMC prototype .(25)	45
Figure 23 Diamond dipole antenna.	46
Figure 24 Final antenna with hybrid reflector.	46
Figure 25 Geometry of the three types of slot antennas. (a) Slot antenna1, (b) Slot antenna2 and (c) the proposed structure	47
Figure 26 Top and side views of the composite antenna. (27)	47
Figure 27 Dimensions of bowtie + balun: (a) Top view and (b) Bottom view (28).....	51
Figure 28 AMC cell.....	52
Figure 29 Boundary conditions of the AMC structure.	52
Figure 30 Boundary conditions of a structure.	53
Figure 31 Far filed distance in Wave guide port	53
Figure 32 Phase reflection coefficient.....	54
Figure 33 Bowtie antenna over AMC with 8*8 cells: (a) Front view, (b) side view.	55
Figure 34 Reflection Coefficient S_{11}	55
Figure 35 Broadside realized gain of 8x8 AMC-based antenna and without AMC.....	56
Figure 36 current distribution in AMC 8x8 at: 4 GHz, 8GHz and 12 GHz	57
Figure 37 Dimensions of the overall structure (bowtie + balloon at AMC with 8*5 cells): (a) Top view and (b) Bottom view	57
Figure 38 :Reflection coefficient of the variation of the parameter L_{cps}	58
Figure 39 Gain en broad side of the variation of the parameter L_{cps}	58

Figure 40 Reflection coefficient of the variation of parameter L_p	59
Figure 41 Gain en broad side of the variation of parameter L_p	59
Figure 42:Reflection coefficient of the variation of parameter W_p	60
Figure 43 :Gain en broad side of the variation of parameter W_p	60
Figure 44: Reflection coefficient of the variation of parameter W_{add}	61
Figure 45 Gain en broad side of the variation of parameter W_{add}	61
Figure 46 :Reflection coefficient of the variation of number of Vias	62
Figure 47: Gain en broad side of the variation of number of Vias	62
Figure 48: Reflection coefficient of the optimized structure.....	63
Figure 49: Realized gain vs. frequency in the broadside direction.	64
Figure 50 : Current distribution at 4 GHz	64
Figure 51 : Current distribution at 6 GHz	64
Figure 52: The directive radiations patterns of the optimized structure a t 4.08 GHz, 4.7 GHz, 5.28 GHz, 5.8 GHz and 6.4 GHz.....	65

Abbreviations

AMC : artificial magnetic conductors
AS: Authorized Service
BALUN: Balanced to Unbalanced
BDS: BeiDou Navigation Satellite System
BOC : Binary Offset Carrier
BOC : Binary Offset Carrier
BPSK :Binary Phase-Shift Keying
BSS: Broadcast Satellite Services
CDMA: Code Division Multiple Access
CPW : coplanar waveguide
CST : Computer Simulation Technology
CS : Commercial Service
DARS : Digital Audio Radio Services
DBS: Direct Broadcast Service
DNG: Double negative
DTH: Direct to Home Internet Services
EBG: Electromagnetic band gap
EU :Europe
EIRP :Effective Isotropic Radiated Power
FDMA: Frequency Division Multiple Access
FM: Frequency Modulation
FIT: Finite Integral Technique
FSS : Fixed Satellite Services
HPA: High Power Amplifier
IF :Intermediate Frequency

GNSS: Global Navigation Satellite System
GLONASS: Global'naya Navigatsionnaya Sputnikovaya Sistema
GPS: Global Positioning Service
GEO: Geostationary Earth Orbit
GLONASS: GLObal'naya NAVigatsionnaya Sputnikkovaya Sistema
LH: Left-handed
LNA : Low Noise Amplifier
MEO: Medium Earth Orbits
MPA: microstrip patch antenna
NRI: Negative refractive index
OS :OpenService
PEC : perfect electric conductor
PPS :Precise Positioning Service
PRS: Public Regulated Service
PNT: Positioning, Navigation and Timing
PMC: perfect magnetic conductor
PSK : Phase Shift Keying
RF: Radio Frequency
RFID: Radio Frequency Identification
RHCP: have right hand circularly polarized
SPS: Standard Positioning Service
TE : Transverse Electric
TM: Transverse Magnetic
TMBOC : Time Multiplexed Binary Offset Carrier
UHF: Ultra High Frequency
UWB: Ultra-wideband radio
VHF: Very High Frequency

Introduction

High-speed data transmission, linked to the ever-increasing demand for mobile devices, has generated great interest for microstrip antennas, which are antennas most used in compact commercial designs. The main advantages of these antennas are the low weight; low volume and thickness, low cost, simplicity of manufacture. However, this type of elements has limitations, including narrow bandwidth, low gain and the ability to resonate with a single frequency.

An antenna with radiating elements, commonly called "patch antenna", is a micro-ribbon line of particular shape. It is important in relation to communications devices (the transmitter and receiver), and in other words is the designer for transporting and emitting electromagnetic waves. It is also used in systems such as radiocommunications, communications networks, satellites and detection systems and civil aviation and radars.

The rapid development of telecommunications systems has made it possible to create and innovate several technologies. On the one hand, there is a trend toward miniaturization of mobile device related components. On the other hand, there is a growing demand for fast data transfer which in turn requires broadband and / or multiband components. These two constraints contradictory needs to be overcome with inexpensive and high performance solutions.

One of the solutions proposed to meet these needs is the exploitation of the new class of materials known as "meta materials" or Electromagnetic Band Gap "EBG".

EBG are artificial composite materials whose internal structure is often periodic and can exhibit great advantages over conventional solutions like antennas with metallic reflectors. A reflector made up of perfect electrical conductor (PEC) needs to be placed at a distance of $\lambda/4$, λ being the wavelength at the central frequency of operation, in order to avoid the destructive interference between the incident and reflected electric fields in the broadside direction. This leads to a thick antenna profile. Metamaterials like AMC can be used instead to reduce the thickness of the antenna. Metamaterials are artificially engineered materials that exhibit exotic properties not found in natural materials. These properties originate from their structure and not from their composition.

The objective of this work is to design low profile wideband antenna with metamaterials. These structures can be used in order to improve antennas by reducing their thickness and making them unidirectional rather than bidirectional. Thus, designing unidirectional antennas is required on many platforms (satellite, aircrafts, Unmanned Aerial Vehicle...) in order to obtain outward radiation and preserve the interior of any electromagnetic pollution. Furthermore, for integration and mechanical constraints, antennas have to be low profile.

The first chapter is about Global navigation and communication satellite system with brief overview on antennas for space applications..

The second chapter reviews principal's properties and applications of EBG in antennas. Also we developed a state of the art on wideband antennas using an artificial magnetic conductor.

The objective of the third chapter is to design a directive wideband, low profile bowtie antenna by using AMC reflectors which operates in the C band.

Finally, a conclusion and perspectives of this work are presented.

CHAPTER I

Satellite System for navigation and communication

Chapter I: Satellite System For navigation and communication

I.1 introduction

Satellite-based technologies are the enabling tools for a wide range of civil, military and scientific applications, like communications, navigation and timing, remote sensing, meteorology, reconnaissance, search and rescue, space exploration and astronomy. In order to formulate a clear view on our research topic we focused on global navigation satellite system and communication satellite system.

I.2 Global Navigation Satellite Systems

Global navigation satellite system (GNSS) is a general term describing any satellite constellation that provides positioning, navigation, and timing (PNT) services on a global or regional basis, GNSS is used for many types of applications, covering the mass market, professional and safety-critical applications as well as a whole range of scientific applications, There are therefore literally hundreds of applications of GNSS, from the everyday to the exotic, as shown in Figure 1.

While GPS is the most prevalent GNSS, other nations are fielding, or have fielded, their own systems to provide complementary, independent PNT capability. In this regard, the European nations are developing the Galileo system, the Russians are modernizing their GLONASS system while the Chinese are launching a new Compass system. All of these systems form GNSS with desirable positional capability suitable for mining operations and civil engineering tasks. These GNSS desirable capabilities are(1):

- Global:** This enables their use anywhere on earth.
- All weather:** This feature makes GNSS useful during cloudy and rainy periods.
- Able to provide 24-hour coverage:** This enables both day and night observation and can thus enable, e.g., rescue mission in mine operations to be undertaken at any time.

-Cheaper: Compared to other terrestrial surveying observation techniques such as leveling and traversing, GNSS are economical due to the fact that as an operation, few operators are needed to operate the receivers and process data. Less time is therefore required to undertake.



Figure 1: Examples of everyday GNSS applications (1)

1.2.1 Current global navigation satellite system

Currently, there are four global navigation satellite systems in operation, GPS (US), GLONASS (Russia), BeiDou (China), and Galileo (EU) they commonly consist of three components(2):

_ **The space segment** comprises a constellation of satellites orbiting above the Earth's surface that transmit ranging signals on at least two frequencies in the microwave part of the radio spectrum.

_ **The control segment** is responsible for maintaining the health of the system by monitoring the broadcast signals and computing and uploading to the satellites required navigation data. It consists of a group of globally (or locally)-dispersed monitoring stations, ground antennas for communicating with the satellites, and a master control station with a backup facility at a different location.

– **The user segment** consists of GNSS receiving equipment both civil and military. This includes receivers on the ground, at sea, in the air, and even in space.

For an overview summary see table I.1

System	GPS	GLONASS	BeiDou	Galileo
				
Orbit	MOE	MOE	MEO IGSO	MEO
Nominal Number of satellite	24	24	27,3,5	30
Constellation	6 planes 56° inclination	Walker(24/3/1) 64.8°inclination	Walker(24/3/1), 55°inclination	Walker (24/3/1), 56° inclination
Service	SPS, PPS	SPS, PPS	OS,AS, WADS,SMS	OS,CS, PRS
Initial service	Dec 1993	Sep 1993	Dec 2012	2016/2017 planned
origin	USA	Russia	China	Europe
coverage	Global	Global	Global	Global
Frequency (MHz)	L1 1575.42	L1 1602.00	B1 1561.098	E1 1575.42
	L2 1227.60	L2 1246.00	B2 1207.14	E5a 1176.45
	L5 1176.45	L3 1202.025	B3 1268.52	E5b 1207.14
				E61278.7

Table 1: An overview of the global satellite-based navigation systems.

I.2.2 GNSS signals

Each satellite system has specific signal characteristic, but each system attempts to be compatible with others in order to prevent interferences and attenuation between the signals.

a) GPS:

The GPS system is used by more than one trillion of users and transmits 4 civilian signals(3) :

- L1C/A at 1575.42 MHz it is called the legacy signal and broadcast by all the satellites ,it use BPSK(1) modulation

– L2C at 1227.6 it is the second civilian-use signal with BPSK modulation

– L5 at 1176.45 MHz for aviation safety of life signal using BPSK(10)

– L1C at 1575.42 for international signal using TMBOC(6.1.1/11) modulation

also the GPS satellites transmit signals for the military use.

b) BeiDou Navigation Satellite System (BDS):

The BeiDou Navigation Satellite System (BDS) is a new family member in the Global Navigation Satellite System(GNSS). It increases the usability and availability of Positioning, Navigation and Timing (PNT) around China in Asia Pacific area, and the global users can also profit from the constellation for high accuracy(4). The satellites transmit two levels of service, an open service and an authorized service primarily for the Chinese government and military using three frequency bands. The bands and the central frequencies for the satellites now in use, the BeiDou-2 satellites, are B1 at 1561.098MHz, B2 at 1207.14MHz, and B3 at 1268.52MHz.

c) Galileo:

Galileo is the European Union's Global Satellite Navigation System (GNSS). Sometimes called the 'European GPS', Galileo provides accurate positioning and timing information. Galileo is a programme under civilian control and its data can be used for a broad range of

applications. It is autonomous but also interoperable with existing satellite navigation systems.

Galileo satellites transmit three levels of service in three frequency bands using CDMA(2). The Open Service (OS) and the Public Regulated Service (PRS) are transmitted in the E1 frequency band centered on 1575.46MHz (the same as the GPS L1 frequency) and the PRN ranging codes are modulated onto the carrier using binary offset carrier (BOC) techniques with each satellite, like GPS, assigned separate codes. The Commercial Service (CS) signal and the PRS are transmitted in the E6 frequency band centered on 1278.75MHz using binary phase-shift keying (BPSK) and BOC modulation, respectively. Data and data-less (pilot) signals are transmitted in the E5 frequency band centered on 1191.795MHz using BOC modulation. Data and pilot signals are also available on E1 and E6. The signals are separated into an E5a and an E5b component and either can be tracked separately or together. The various signals also contain navigation messages supplying the necessary information for acquiring Galileo signals and for determining receiver positions and time.

d) GLONASS:

The former Soviet Union developed the *Global'naya Navigatsionnaya Sputnikovaya Sistema* or GLONASS, GLONASS uses frequency division multiple access (FDMA) for its signals. Originally, the system transmitted the signals within two bands: L1, 1602–1615.5MHz, and L2, 1246–1256.5MHz, at frequencies spaced by 0.5625MHz at L1 and by 0.4375MHz at L2. GLONASS-K satellites include, for the first time, code division multiple access (CDMA) signals accompanying the legacy FDMA signals. GLONASS-K1 as well as the latest GLONASS-M satellites transmit a CDMA signal on a new L3 frequency (1202.025MHz).(2)

I.2.3 Measuring principle

Position is calculated by accurately measuring the distance of a receiver from the satellite by determining the delay in the radio signal transmitted by the satellite. This delay is measured by matching and comparing the received signals by an equivalent receive generated signal more precise measurements use phase instead of timing measurements(5). The starting point is the basic principle of physique that relate the travel time t , distance travelled d and speed of light c , namely:

$$\text{Distance } (d) = \text{speed}(c) \times \text{time } (t)$$

If time can be accurately measured and the speed c is known, then it is possible to obtain the distance d this basic expression forms the foundation of GPS satellite positioning GPS receiver situated on a ground or on a space accurately measure the time t taken by the signal travel from the satellite to the receiver.

Knowing the speed of light (3×10^8 m/s), the distance from the satellite to the receiver known as (pseudoranges) can be measured since the GPS satellite orbit at about 20,000km above the earth it takes around 0.07s for the signal to travel from the satellite to the receiver

The satellite generate a binary code (C/A and P) that are sent to the receiver witch generate identical binary codes, the receiver generated code are then compared to those received from the satellite, witch lag behind those generated by the receiver, by comparing the two signal (from the satellite and the receiver), the receivers are able to compute the travel time of the signal.

A binary code generated by the satellite takes the form of +1/ -1 in order to measure the time travelled by the signal accurately, the receiver and satellite clocks must be synchronized and error free, the clocks normally have errors that are propagated to the measured ranges.

The measuring principle valid for all the other GNSS systems, they only differ in design, signal structure and coordinate systems.

I.3.Satellite Communication Systems

In satellite communication (Figure 2), satellites are used to relay signals between ground stations. The signal is received from one ground station and re-transmits to one or more receiving ground stations elsewhere with the help of satellite. In this process, signal from ground station is first sent towards the satellite, then amplifies the signal and sends it back to the other ground station. As the signal is transferred through space, this kind of communication is also known as space communication.(6)

Communications satellites are commonplace in modern society. Applications include television broadcast, mobile telephone networks and data transmission. The convention is to subdivide the satellites by their communications mission.

Each mission is characterized by the service that it provides, the number of users it can support and the geographic area over which the service is provided. Additional features include the connectivity that it offers to its users, the spectrum that it is allocated, the power

levels that are used, the scheme by which multiple users can share the satellite resource and the ability of the satellite to be reconfigured.

The major mission categories are Fixed Satellite Services (FSS), Broadcast Satellite Services (BSS), Digital Audio Radio Services (DARS), Direct to Home Internet Services (DTH) and Mobile Communications Services (Mobile). Sometimes BSS systems are referred to as Direct Broadcast Service (DBS) systems.



Figure 2 Satellite communication(6)

I.3.1 Satellite Communications Spectrum

The three most commonly used satellite frequency band are the C-, Ku- and Ka-bands. The C-band is the oldest allocation and uses around 6 GHz for transmission (uplink) and between 3.7 and 4.2 GHz for reception (downlink).

Ku-band is the most prevalent transmission format for satellite TV in Europe and uses around 14 GHz for uplink and between 10.9 and 12.75 GHz for the downlink.

Ka-band uses around 30 GHz up- and between 18 and 20 GHz downlink frequency. The highest frequency band typically gives access to the broader bandwidths, but is also more vulnerable to signal degradation due to 'rain fade(6)'.

There are other frequency bands available in satellite communication like VHF, UHF, L, and S for an overview (table 2).

Band	Frequency		Bandwidth	Application
VHF	<200 MHz			messaging
UHF	200 MHz – 1 GHz			Messaging, positioning, voice and fax
L	2/1 GHz			Mobile satellite services(MSS)
S	4/2.5 GHz			Fixed satellite services (FSS)
	Frequency(GHz)			
	uplink	downlink		
C	5.9-6.4	3.7-4.2	500 MHz	Fixed point to point ground station
X	7.9-8.4	7.25-7.75	500 MHz	Mobile ,radio relay ,military only
Ku	14-14.5	11.7-12.2	500 MHz	Broadcast, fixed point services not military
Ka	27.5-31	17.7-21.2	3.5 GHz	

Table 2: Satellite bandwidth and applications.

1.3.2 Elements of Satellite Communications System

The two major elements of the satellite communications system are: the space segment and the ground segment with earth stations, communication links, user terminals and interfaces and network control center. The earth stations are most often connected to the end users terminal through the terrestrial network or in case of small station connected to the end user terminal directly. The function of the earth station is to transmit a signal to the satellite and receive a signal from the satellite(7).

The block diagram of satellite communication system is shown in Figures 3 and 4.

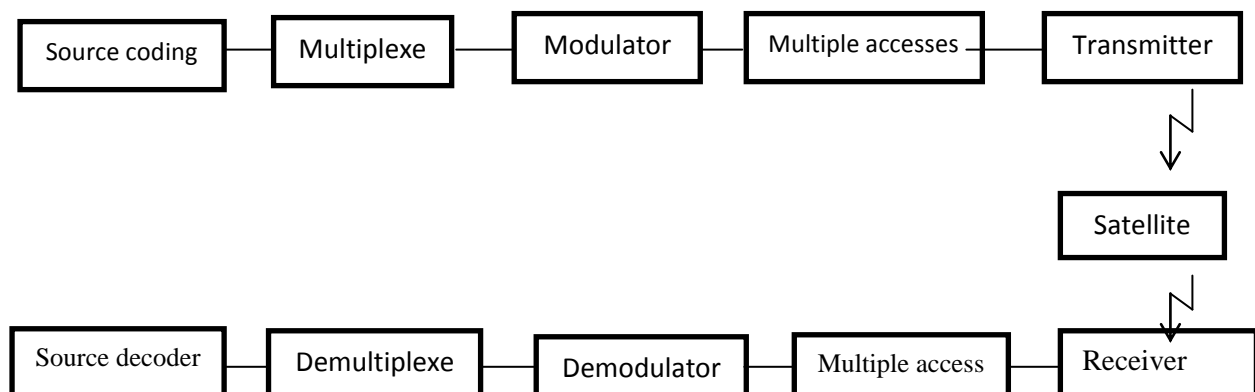


Figure 3: Signal processing elements in satellite communications.

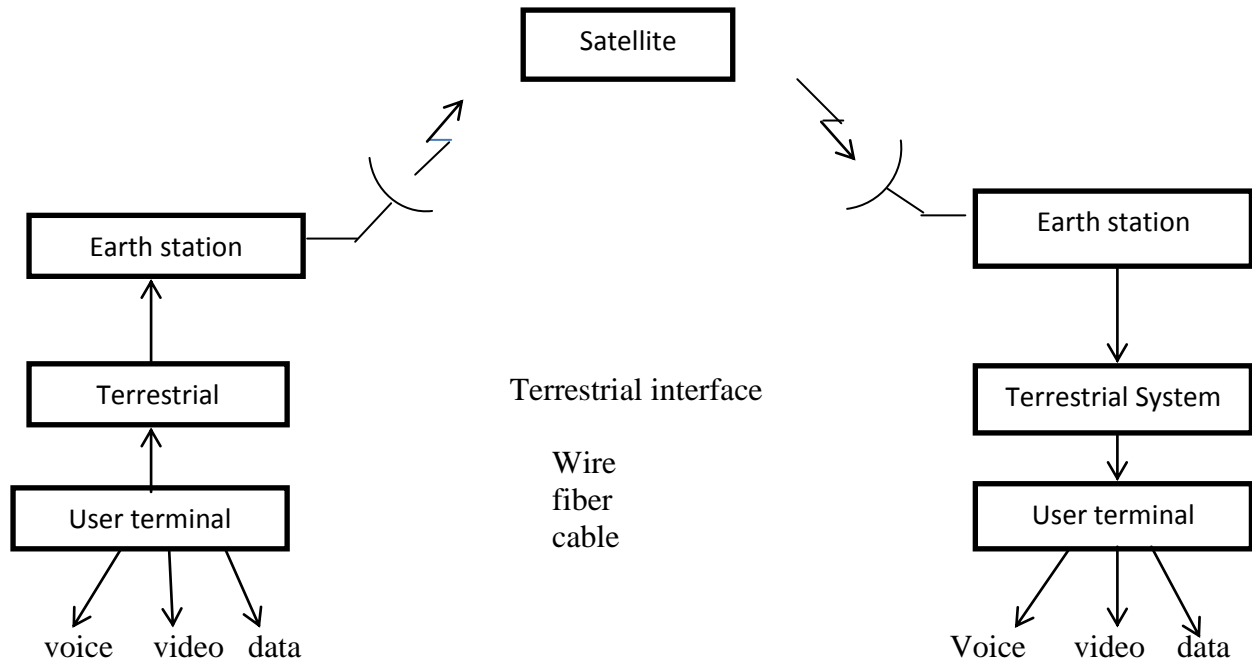


Figure 4: Element of satellite communication system.

a) Space Segment:

The space segment comprises of satellite and the equipment on board of the satellite. The satellite consists of the payload and the subsystems. The payload consists of the receiving and transmitting antennas and all the electronic equipment which holds the transmission of the carriers(6). Communication satellites are complex and expensive to acquire and launch. The Placement of a satellite into the orbit and operating it for 12 or more years involves a great deal. Placement in orbit is accomplished by contracting with a spacecraft manufacturer and launch agency and allowing them about three years to design, construct, and launch the satellite. The mass and volume of the electric power supply of a satellite poses one of the most restricting problems. In some applications such as television broadcasting or mobile and personal communications, the required electric power is over 10 kW which results in large weight and volume for communications satellites. Therefore, lightweight material is used for optimal design to support the load, withstand vibration and to keep the size and weight of the satellite small. Large temperature cycles are opted for the structure of the satellite. Once the satellite is placed in the proper orbit, it becomes the responsibility of a satellite operator to control the satellite for the duration of its mission. It is fairly complex task and involves both sophisticated ground-based facilities as well as highly trained technical personnel.

Satellite Payload:

The payload in most commercial communication satellites consists of two distinct parts the transponder and the antennas.

a) Transponder:

There are two basic types of satellite transponders: repeater or bent pipe and processing or regenerative. In the repeater type, communication transponder captures the signals from earth, merely amplifies and frequency shifts the signals, whereas, in processing transponder, the RF carrier is demodulated to baseband signal and process the signals and later re-modulated the baseband signal in addition to frequency translation and amplification(6).

-Analog communication systems are entirely repeater type.

-Digital communication system may use any type. Figure 5 a, b shows the schematic diagrams of repeater type and regenerative type transponders respectively.

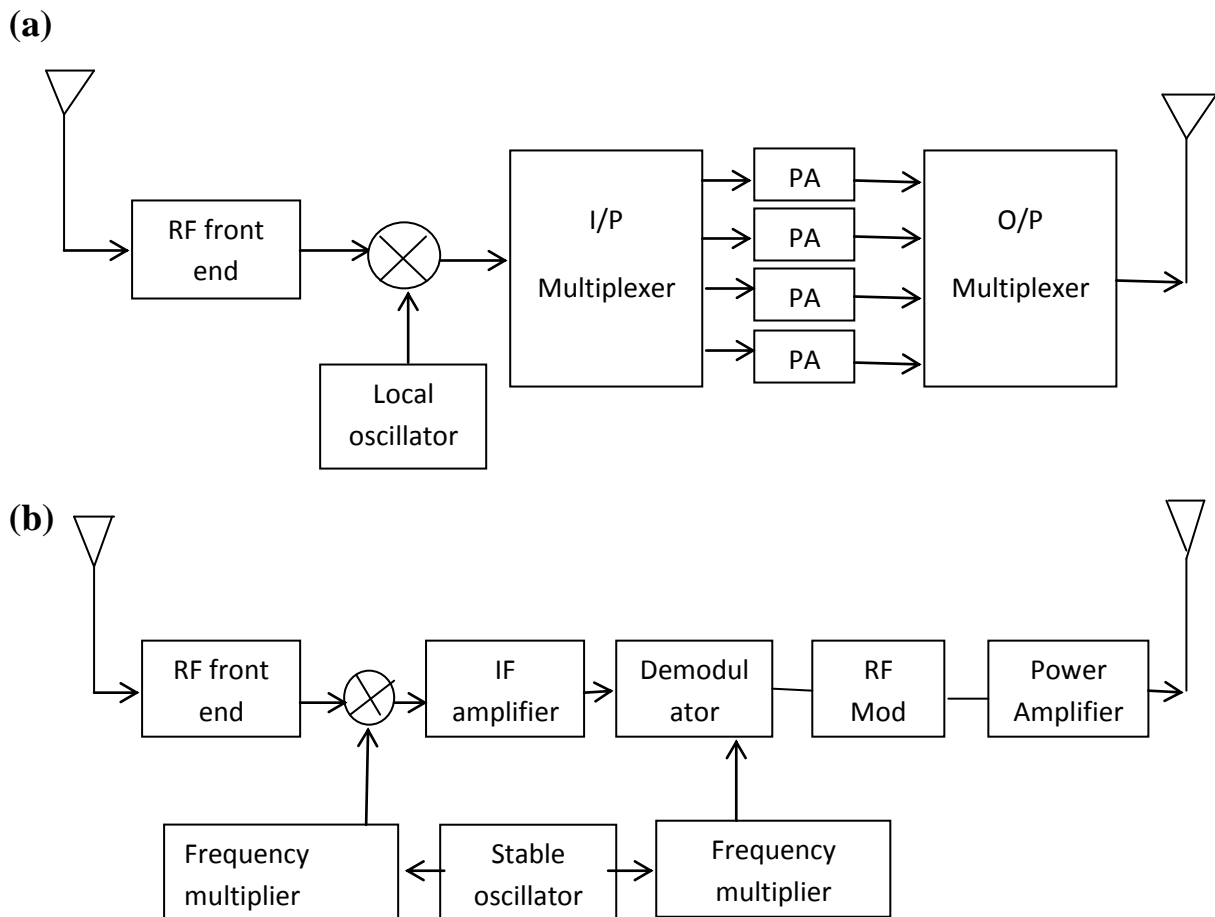


Figure 5: Repeater transponder. b Regenerative transponder

b) Satellite antennas:

The Satellite station receives and retransmits the signals using satellite antennas which maintain the link between the ground segment and the communication transponder. The size and shape of the satellite antennas depend on the specific coverage requirements of the system. Satellite antennas generate small multiple spotbeams and increase the EIRP for the same HPA power. Each beam covers a certain portion on the earth surface called footprint. The gain of the satellite antennas is same both in transmission as well as reception because the generated beam widths are same. This necessitates two separate antennas on the satellite but the diameters of the antennas will not be the same (depends on uplink and downlink frequencies). The beam width of a satellite antenna is equal to or less than the angle of view of the earth from the satellite, which is 17.5° in case of a geostationary satellite. The core functionalities of satellite antennas are as follows:

- **To capture the radio waves**, that is transmitted from ground station at uplink frequency band and with a given polarization; to capture the desirable signals and reject undesired signals as possible.
- **To transmit radio waves**, in a given downlink frequency band and with a given polarization, to a specific region on the earth surface.
- **To transmit more focused power** i.e., reduce wastage of power antennas for Satellite Communication.

The antennas on board the satellite serve as an interface between the Earth stations on the ground and various satellite sub-systems during operations. Antennas receive the uplink signal and transmit to downlink signals. In addition they provide single link for the satellite telemetry, command and ranging systems which in conjunction with attitude control subsystem provides beacon tracking signals for precise pointing of the antenna towards the Earth coverage areas. The design of satellite antenna is conditioned by the required coverage. It should be remembered that antennas are the one of the key elements in a satellite communication system since their gain values directly determine the amount of received power.

b) Ground Segment

The ground segment of satellite communication system supports the space segment and has a command (uplink) function as well as data (telemetry and mission function). It sets up the communications links between the satellite and the user. In large and medium system, the terrestrial microwave link interfaces with the user and the earth station. However, in the case of small systems, the end user's terminal interface is located at the earth station. The earth station (Figure 6) consists of:

- Transmit equipment.
- Receive equipment.
- Antenna system.

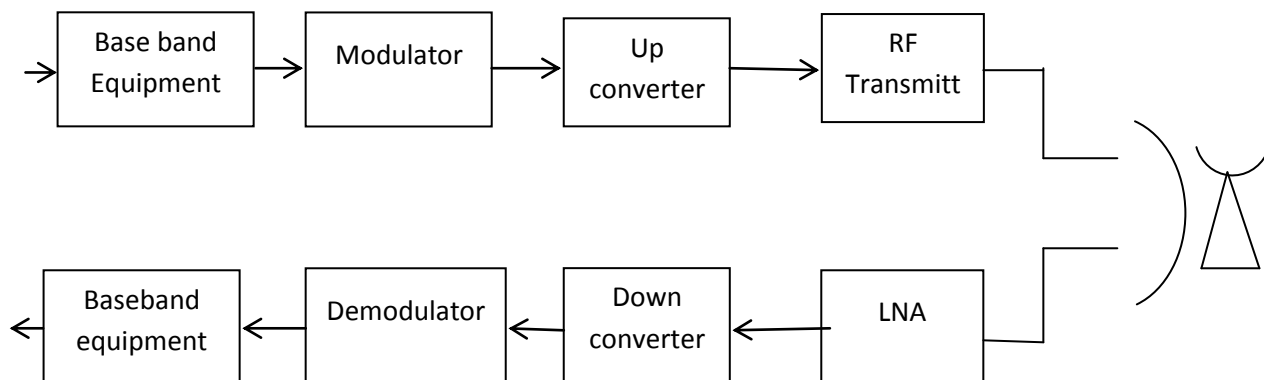


Figure 6: Shows a schematic block diagram of an earth station

In the ground station, the base band signal of terrestrial network is modulated on IF and then up-converted before transmitting to the satellite. The receiving ground station transmits the base band signal to the user directly or through the terrestrial link.

The baseband signals received at the earth stations are generally telephone, television or data signals. It can relay information from a single source or from several sources through multiplexing of signals from the individual sources. In early days, FM modulation scheme is used for analog voice and video signal transmission in satellite communications. Now, the transmission signal is mostly digital for both voice and video and the modulation schemes such as phase shift keying (PSK) and frequency shift keying (FSK) are implemented for transmission.

The monitoring, alarm and control equipment of the earth station has the following purposes:

- To monitor the network operations and controlling the station and managing the traffic.

- To give alarms in case of inaccurate operation or an occasion that affects the main station equipment or the link performance and allow detection of the equipment which is involved.
- To control the station equipment including adjustment of parameters, switching of redundant equipment and so on, it should keep in mind that the correct functioning of network operations and control center is necessary where the number of users in the network is large.

I.4 Various Types of Antenna with Respect to their Applications (antennas for space applications)

Antenna is the most important part in wireless communication systems. Antenna transforms electrical signals into radio waves and vice versa. The antennas are of various kinds and having different characteristics according to the need of signal transmission and reception(8)

1.4.1 Microstrip Patch Antenna:

Microstrip patch antennas (MPA) are well known for their performance and their robust design, (Figure 7), fabrication and their extent usage. The advantages of this Microstrip patch antenna are to overcome their de-merits such as easy to design, light weight etc., the applications are in the various fields such as in the medical applications, Mobile and satellite communication application , Global Positioning System applications and of course even in the military systems just like in the rockets, aircrafts missiles etc. . It is also expected that due to the increasing usage of the patch antennas in the wide range this could take over the usage of the conventional antennas for the maximum applications(9) .

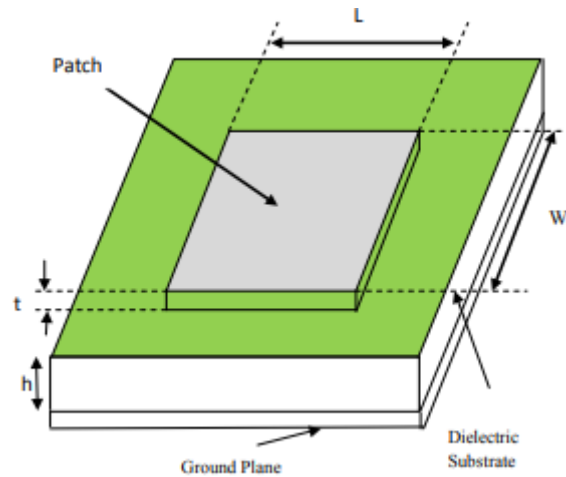


Figure 7: Example of patch antenna.

I.4.2 spiral antenna

Spirals antennas belong to the class of the so called frequency independent antennas, (Figure 8) .Due to their self-invariant scalability it is possible to cover a wide range of frequencies, from 3.1 to 10.6 GHz is indicated Ultra-wideband radio (UWB)(10) . The benefit of spiral antenna is its simple manufacturing, led expenditure, long life, and higher emission performance(11).

The spiral antennas have various applications, in wireless communication due to their high bandwidth(12) also it used inGNSS (GPS), where it is advantageous to have right hand circularly polarized (RHCP) antennas.



Figure 8: Representation of spiral antenna (11).

I.4.3 Helical antenna

A helical antenna is a helical shaped conductor wound around a cylinder,(Figure 9). This antenna can radiate in different modes but the axial mode is one of the most commonly used that because it gives maximum radiation power, Some of the advantages of the helix antennas include their wide bandwidths, easy implementation, real input impedances and circularly polarized fields(13) . Helical antennas have been used in many applications and for different frequency bands; they are the most widely proposed antennas in satellite communications systems.

The main reason why these antennas constitute an asset in applications concerning satellite and space communications generally is circular polarization.



Figure 9: Helical antenna;

I.4.4 Phased array antenna

A phased array antenna is composed of lots of radiating elements each with a phase shifter. Beams are formed by shifting the phase of the signal emitted from each radiating element, to provide constructive/destructive interference so as to steer the beams in the desired direction.

Phased array antennas are becoming increasingly popular in satellite communications because of their inherent advantages of beam reconfigurability(14).

Various applications of phased array antennas including target identification communication.

With the recent advancement of solid state technology and fabrication process the phased array antennas are becoming cost effective and gaining importance due to much flexibility it offers.

I.4.5 Mesh reflector:

Deployable mesh reflectors have been successfully used in telecommunications applications for several decades, as shown in Figure 10. The structures are lightweight and can be packaged in a compact form for launch. Once deployed, the antennas are rigid and can be built with surfaces accurate enough for Ka-band operation. Reflector mesh fabrics are available that are fine enough to be highly reflective at Ka-band, yet have relatively low mass(15).

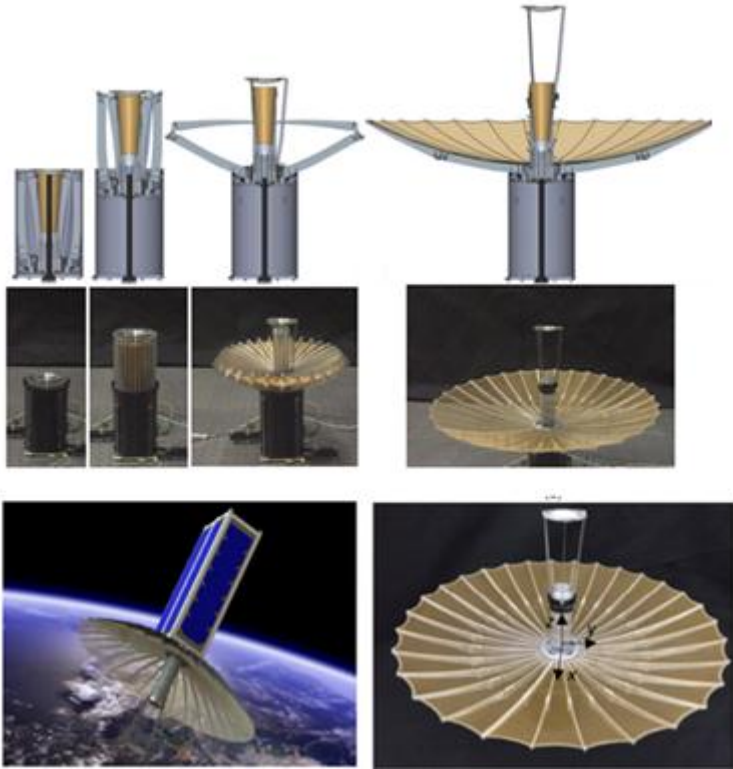


Figure 10: Mesh reflector used in cubesat for Earth Science and Deep Space mission(16)

I.4 Conclusion

In both satellite communication system and navigation satellite system there are a lot of applications that need a high frequency band that means many antennas are required. Employing individual antennas for reception of each frequency, it will be quite costly in addition to increased complexity of the complete system. Therefore, this necessitates the development of multi-frequency or wide frequency band antennas, and that what we are interested in the next chapters.

CHAPTER II

EBG structure and state of the art on
wideband antenna with Artificial Magnetic
Conductor

Chapter II:EBG structure and state of the art on wideband antenna with Artificial Magnetic Conductor

II.1 Introduction

In this chapter, we will focus on the definition of EBG structure, their characteristics and applications that have been developed with antennas. Then, we will draw up a state of the art on wideband antennas using the artificial magnetic reflector.

II.2 Background

Antenna designs have experienced enormous advances in the past several decades and they are still undergoing monumental developments (17). Many new technologies have emerged in the modern antenna design arena and one exciting breakthrough is the discovery/ development of electromagnetic band gap (EBG) structures. The applications of EBG structures in antenna designs have become a thrilling topic for antenna scientists and engineers.

The recent explosion in antenna developments has been fueled by the increasing popularity of wireless communication systems and devices. From the traditional radio and TV broadcast systems to the advanced satellite system and wireless local area networks, wireless communications have evolved into an indispensable part of people's daily lives.

Antennas play a paramount role in the development of modern wireless communication devices, ranging from cell phones to portable GPS navigators, and from the network cards of laptops to the receivers of satellite TVs. A series of design requirements, such as low profile, compact size, broad bandwidth, and multiple functionalities, keep on challenging antenna researchers and propelling the development of new antennas.

Electromagnetic band gap (EBG) structures and their applications in antennas have become a new research direction in the antenna community. It was first proposed to respond to some antenna challenges in wireless communications.

For example:

_ How to suppress surface waves in the antenna ground plane? Or , how to design an efficient low profile antenna near a ground plane?

II.3 EBG definition

EBG structures are usually realized by periodic arrangement of dielectric materials and metallic conductors. In general, they can be categorized into three groups according to their geometric configuration: three-dimensional volumetric structures, two-dimensional planar surfaces, and one-dimensional shown in Figure 11.

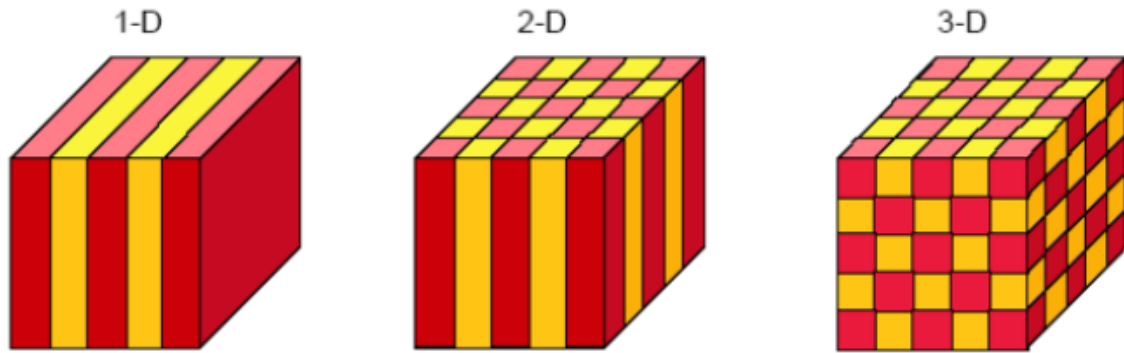


Figure 11: Periodic structure 1D, 2D, 3D(18)

Almost at the same time, another terminology, “*metamaterials*,” also appeared and has become popular in the electromagnetics community (18). The ancient Greek prefix, *meta*(meaning “beyond”), has been used to describe composite materials with unique features not readily available in nature. Depending on the exhibited electromagnetic properties, various names have been introduced in the literature, including:

- _ *Double negative (DNG) materials* with both negative permittivity and permeability.
- _ *Left-handed (LH) materials* inside which the electric field direction, magnetic field direction, and propagation direction satisfy a left-hand relation.
- _ *Negative refractive index (NRI) materials* that have a negative refractive index;
- _ *Magneto materials* with artificially controlled high permeability;
- _ *Soft and hard surfaces* that stop or support the propagation of waves;
- _ *High impedance surfaces* with relatively large surface impedances for both TE and TM waves;
- _ *Artificial magnetic conductors (AMC)* that exhibit the same properties as a perfect magnetic conductor.

Due to their unique band gap features, EBG structures can be regarded as a special type of met materials(18).

Besides the band gap feature, EBG also possesses some other exciting properties, such as high impedance and AMC. For example, a mushroom-like EBG surface exhibits high surface impedances for both TE and TM polarizations. When a plane wave illuminates the EBG surface, an in-phase reflection coefficient is obtained resembling an artificial magnetic conductor. In addition, soft and hard operations of an EBG surface have also been identified in the frequency-wavenumber plane. These interesting features have led to a wide range of applications in antenna engineering, from wire antennas to microstrip antennas, from linearly polarized antennas to circularly polarized antennas, and from the conventional antenna structures to novel surface wave antenna concepts and reconfigurable antenna designs. In summary, electromagnetic band gap structures are an important category of met materials.

II.4 Characterization of EBG structures

To more readily understand the operation of EBG structures, some circuit models have been proposed. A simple two-dimensional planar electromagnetic band gap (EBG) structure, as shown in Figure 12. This structure was originally proposed in (19). The EBG structure consists of four parts: a metal ground plane, a dielectric substrate, periodic metal patches on top of the substrate, and vertical vias connecting the patches to the ground plane. The geometry is similar to the shape of a mushroom.

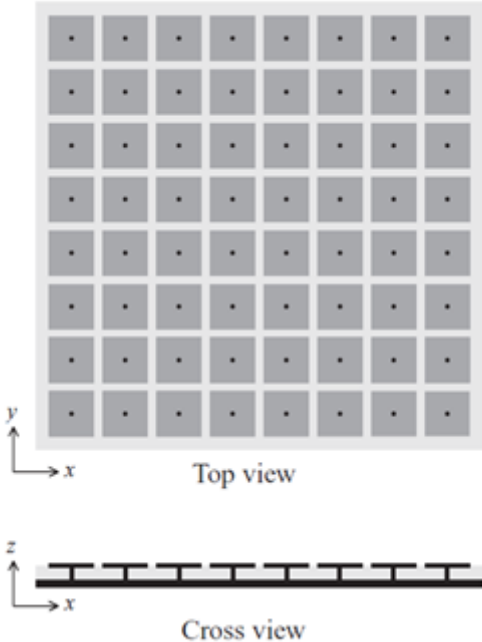


Figure 12: Geometry of mushroom-like electromagnetic band gap (EBG) structure.

The parameters of the EBG structure are labeled in Figure 13.a , as patch width W , gap width g , substrate thickness h , dielectric constant ϵ_r and vias radius r .When the periodicity $(W+g)$ is small compared to the operating wavelength ,the operation mechanism of this EBG structure can be explained using an effective medium model with equivalent lumped LC elements , as shown in Figure 13.b . The capacitor results from the gap between the patches and the inductor results from the current along adjacent patches. The impedance of a parallel resonant LC circuit is given by:

$$Z = \frac{Z_L Z_C}{Z_L + Z_C} = \frac{j L W}{1 - L C W^2} \quad (I)$$



Figure 13: LC model for the mushroom-like EBG structure ; (a) EBG parameter ,(b) model LC.

The resonance frequency of the circuit is calculated as following:

$$f_0 = \frac{1}{2\pi\sqrt{LC}} \quad (II)$$

Near the resonance frequency f_0 , high impedance is obtained and the EBG does not support any surface waves, resulting in a frequency band gap. The high surface impedance also ensures that a plane wave will be reflected without the phase reversal that occurs on a perfect electric conductor (PEC).

The value of the capacitor is given by the fringing capacitance between neighboring coplanar metal plates. This can be derived using conformal mapping, a common technique for determining two-dimensional electrostatic field distributions. The derivation starts with a pair of semi-infinite plates separated by a gap situation is given by the following equation:

$$C = \frac{W\epsilon_0(1+\epsilon_r)}{\pi} \cosh^{-1} \left(\frac{W+g}{g} \right) \quad (III)$$

The value of the inductor is derived from the current loop in Figure 13.b, consisting of the vias and metal sheets. For a solenoid current, the magnetic field can be calculated using Ampere's law. The equivalent inductor is then computed from the stored magnetic field

energy and the excitation current. After a simple derivation, the inductance is expressed as below. This depends only on the thickness of the structure and the permeability:

$$L = \mu_0 \mu_r h \quad (IV)$$

Substituting (III) and (IV) into (I) and (II), the surface impedance and resonant frequency can be computed. Other characteristic parameters, such as the reflection phase can also be derived accordingly.

Besides the surface wave property, EBG structure also exhibit interesting reflection phase behavior, which will be discussed. Reflection coefficient is a popular parameter used to describe the reflection property of an object. It is defined as the ratio of the reflected field over the incident field at the reflecting surface. Usually, it has a complex value with the corresponding magnitude and phase. When a ground plane exists in an analyzed lossless structure, the magnitude is always one because all the energy is reflected back. In this case, the reflection phase is of special interest. With the traditional conductors, if a plane wave is normally impinged upon a perfect electric conductor (PEC), the total tangential E field must be zero in order to satisfy the boundary condition. Thus, the reflected E field and the incident E field should have the opposite signs, resulting in a reflection coefficient of -1 . The reflection phase is 180° for the PEC case. For a perfect magnetic conductor (PMC), the total tangential H field must be zero. Thus, the reflected H field and the incident H field should have the opposite signs whereas the reflected E field and the incident E field have the same signs. As a result, the reflection coefficient is equal to one and the corresponding reflection phase is 0° for PMC case. However, the PMC surface does not exist in nature.

Research on EBG structures reveals that they can realize the PMC condition in a certain frequency band. Thus, they are sometimes referred to as artificial magnetic conductors (AMC). Actually, the reflection phase of an EBG structure is a function of frequency. It varies continuously from 180° to -180° as frequency increases. This reflection phase feature makes EBG surfaces unique and initiates many low profile wire antenna designs on EBG surfaces.

The band gap is defined for a variation of reflection phase between $+90^\circ$ and -90° , white zone in Figure 14.

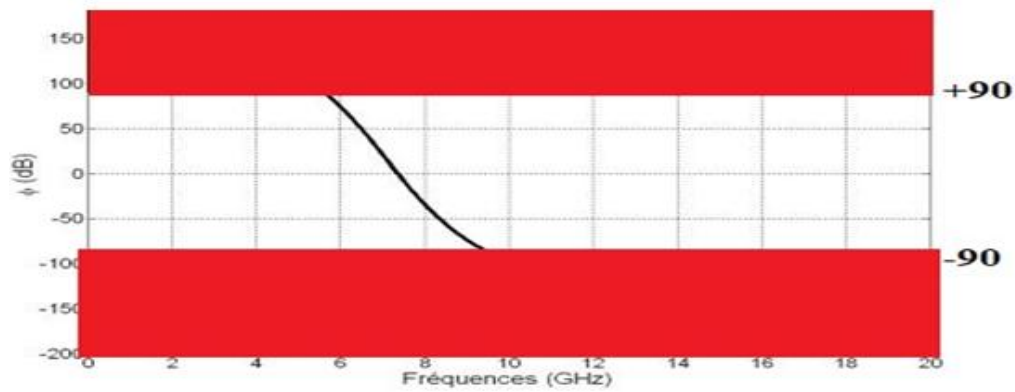


Figure 14: Example of reflection phase.

II.5 EBG applications in antenna engineering

The unique electromagnetic properties of EBG structures have led to a wide range of applications in antenna engineering. This section summarizes several typical EBG applications in antenna designs.

II.5.1 Application for surface wave suppressions

Surface waves are by-products in many antenna designs. Directing electromagnetic wave propagation along the ground plane instead of radiation into free space, the surface waves reduce the antenna efficiency and gain. The diffraction of surface waves increases the back lobe radiations, which may deteriorate the signal to noise ratio in wireless communication systems such as GPS receivers. In addition, surface waves raise the mutual coupling levels in array designs, resulting in the blind scanning angles in phased array systems.

The band gap feature of EBG structures has found useful applications in suppressing the surface waves in various antenna designs. For example, an EBG structure is used to surround a microstrip antenna to increase the antenna gain and reduce the back lobe (20).

In addition, it is used to replace the quarter-wavelength choke rings in GPS antenna designs. Many array antennas also integrate EBG structures to reduce the mutual coupling level. For example, Figure 15 shows a comparison of patch antennas with and without EBG structures and an 8 dB reduction in mutual coupling is observed:

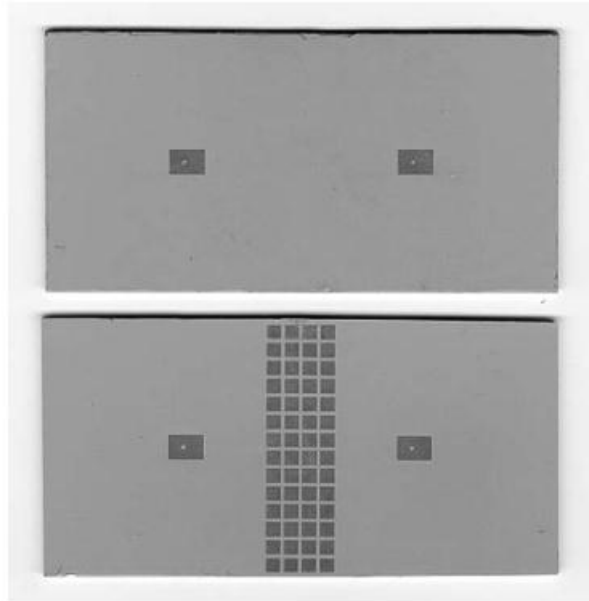


Figure 15: Shows a comparison of patch antennas with and without EBG structures

II.5.2 Application for efficient low profile wire antenna designs

Another favorable application of EBG is to design low profile wire antennas with good radiation efficiency, which is desired in modern wireless communication systems. To illustrate the fundamental principle, Table 3 compares the EBG with the traditional PEC ground plane in wire antenna designs. When an electric current is vertical to a PEC ground plane, the image current has the same direction and reinforces the radiation from the original current. Thus, this antenna has good radiation efficiency, but suffers from relative large antenna height due to the vertical placement of the current. To realize a low profile configuration, one may position a wire antenna horizontally close to the ground plane. However, the problem is the poor radiation efficiency because the opposite image current cancels the radiation from the original current. In contrast, the EBG surface is capable of providing a constructive image current within a certain frequency band, resulting in good radiation efficiency. In summary, the EBG surface exhibits a great potential for low profile efficient wire antenna applications.

Based on this concept, various wire antennas have been constructed on the EBG ground plane (21). Typical configurations include dipole antenna, monopole antenna, and spiral antenna. EBG surfaces have also been optimized to realize better performances such

as multi-band and wideband designs. For example, Figure 16 shown a curl antenna on an EBG structure that radiates circularly polarized radiation patterns.

Options	Efficiency	Low profile
<p>J \uparrow</p> <p>PEC \uparrow</p>	Good	Bad
<p>J \rightarrow</p> <p>PEC \leftarrow</p>	Bad	Good
<p>J \rightarrow</p> <p>EBG \rightarrow</p>	Good	Good

Table 3: Comparisons of conventional PEC and EBG ground planes in wire antenna designs

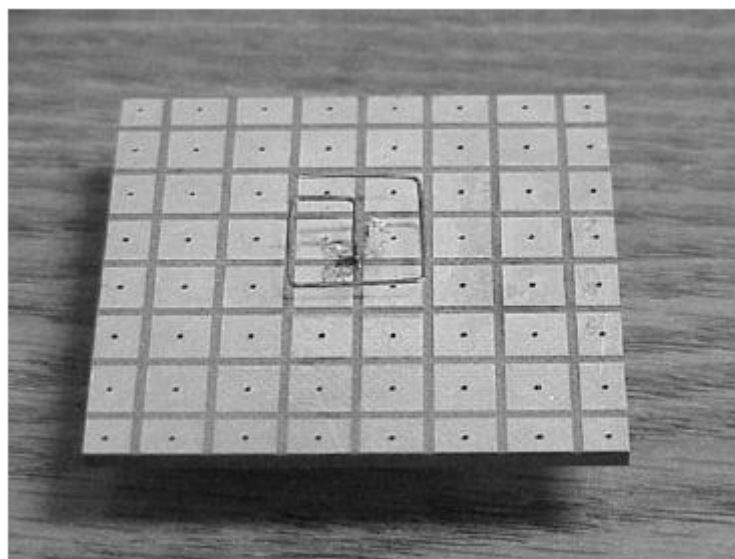


Figure 16: EBG substrate for a low profile curl antenna design (from [24] C _ Wiley InterScience)

II.5.3 Reflection/transmission surfaces for high gain antennas

EBG structures are also applied in designing antennas with a high gain around or above 20 dBi. Traditionally, high gain antennas are realized using either parabolic antennas or large antenna arrays. However, the curved surface of parabolic antennas makes it difficult for them to be conformal with mobile platforms, while large antenna arrays always suffer from loss in

the feeding networks. The planar EBG surfaces provide an alternative solution to this problem. For example, it is used to design a high gain resonator antenna (22), as shown in Figure 17. After optimizing the EBG design, a 19 dBi antenna gain is obtained in the measurement.

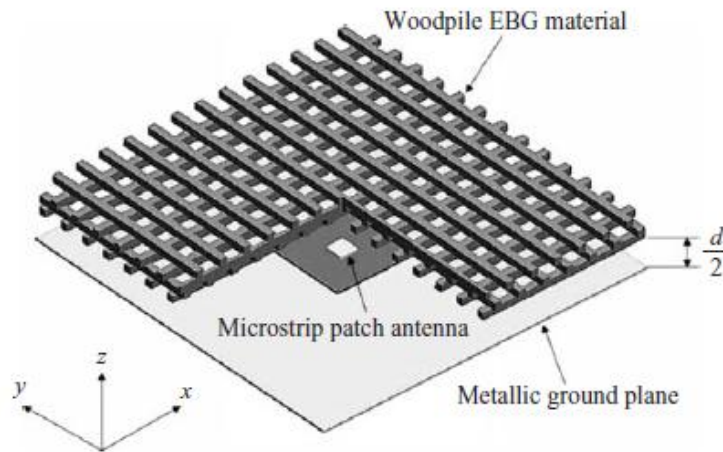


Figure 17: A high gain resonator antenna designs using an EBG structure.

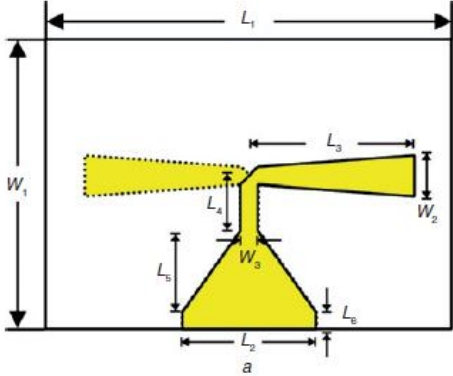
II.6 State of the art on wideband antennas with Artificial Magnetic Conductor

Antennas require being unidirectional for a variety of applications, as shown in Figure 18. For example, an antenna embedded on aircraft or satellite to the outside of the aircraft, while preventing the electromagnetic contamination of its internal environment. To design these antennas with low profile, use of Artificial Magnetic Conductors as reflectors. In addition, multiple functionalities are needed and thus are required. These design requirements, is a real challenge. Therefore, we will focus on the following section on wideband antennas with Artificial Magnetic Conductor

In (23) novel fractal wideband artificial magnetic conductor (AMC) structure is designed as the ground plane of a printed bow-tie antenna for gain enhancement and low profile. The origin printed bow-tie antenna is operated in the range from 1.67 to 2.06 GHz with a trapezoidal balun connected to the SMA. The AMC structure consists of 6×9 first-order fractal unit cells that are made up of four circles and four smaller circles as shown in Figure 19. The distance between the antenna and the AMC is reduced to one-eighth of

the wavelength in free space at 1.7 GHz. The composite antenna has a wide bandwidth from 1.64 to 1.94 GHz, with a relative frequency bandwidth of 16.7%.

The gain is increased, and the maximum gain is 6.5 dBi and the radiation patterns are stable in the whole operating frequency range, which makes it suitable for wireless communication



applications.

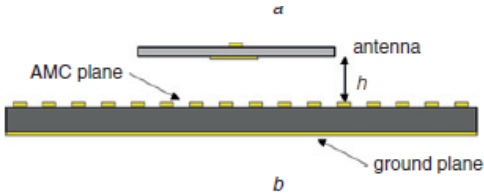


Figure 18: Geometry of Bowtie antenna and composite antenna (23).

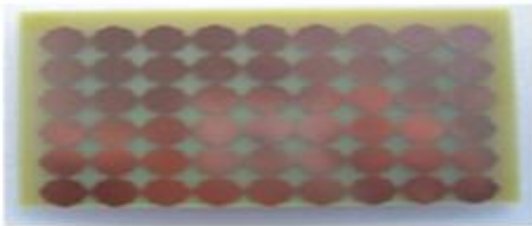


Figure 19: Photograph of fractal AMC plane(23).

In(24)a novel low-profile and highgainantenna which adopts an artificial magnetic conductor(AMC) ground plane as its reflecting surface. Here, the traditional printed dipole

antenna is oriented horizontally over the AMC surface which is consisted of 5*7 square plum-shaped patches unit without vertical via to the ground. The optimized antenna has a height about 9.5mm and its peak gain is closed to 9.7dB at 2.58GHz. Moreover, the operating frequency range is from 2.47GHz to 2.77GHz, its relative bandwidth achieves about 11.63%.

The AMC structure had a 3mm RT/Duroid 6010 dielectric substrate with dielectric constant(equal to 10.2) and the plum-shaped pattern is combined of four symmetrical circular patches and they are designed to be fully symmetrical with $r=2,3$ mm and bandwidth covering from 3,18 GHz to 4,21 GHz .as shown in Figure.20.

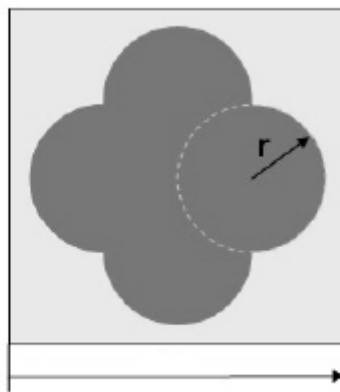


Figure 20: Unit cell of proposed AMC structure.,

The Bowtie antenna presents in Figure.21is etched on a Rogers TMM4(tm) substrate which has a dielectric constant 4.5 and a 0.5mm thickness. The two bowtie arms are on each side of the substrate. The substrate size is 94.15mm (D_x) and 56.625mm (D_y).The length of eachbow-tie arm d is 17.8mm and the long side of the bow-tie patch l_1 is 11mm, the short one, 4mm.

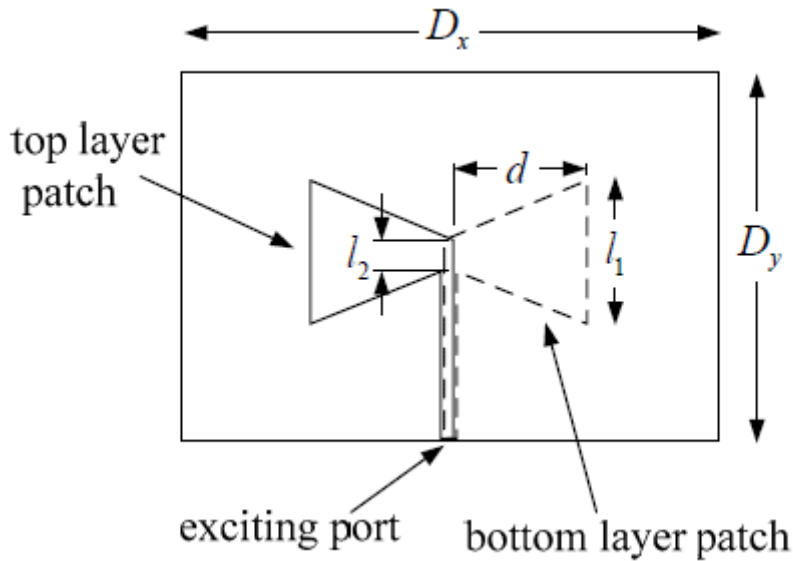


Figure 21: The Bowtie antenna.(24)

The distance between the antenna and the AMC plane is 6 mm which cover a wider bandwidth possible, and the total height of the composite antenna is 9,5m .The frequency range of S_{11} below -10dB is from 2.47GHz to 2.77GHz, which covers the LTE (Long Term Evolution) range from 2.5GHz to 2.69GHz and the peak gain is 9, 67 dB at 2, 58 GHz.

In(25) a novel combination of coplanar waveguide(CPW)-fed double bow-tie slot antenna and artificial magnetic conductor (AMC), which meets the requirements of a 5.8-GHz .SHF RFID tag antenna usable on metallic objects, is presented.

Double Bowtie antenna is used with RO4003C substrate and relative dielectric permittivity $\epsilon_r = 3,38$ and a thickness of $h = 1,524 \text{ mm}$.There is no ground below the dielectric substrate, that is, ungrounded CPW. The AMC structure is a RO4003C substrate with thickness $h = 0,762 \text{ mm}$ and permittivity $\epsilon = 3,38$.As the CPW-fed slot double bow-tie antenna has no ground plane below the dielectric substrate, the AMC's unit cells below the antenna have been removed. The Bow-tie–AMC combination keeps the antenna operating properly in the whole antenna bandwidth. As shown in Figure 22.

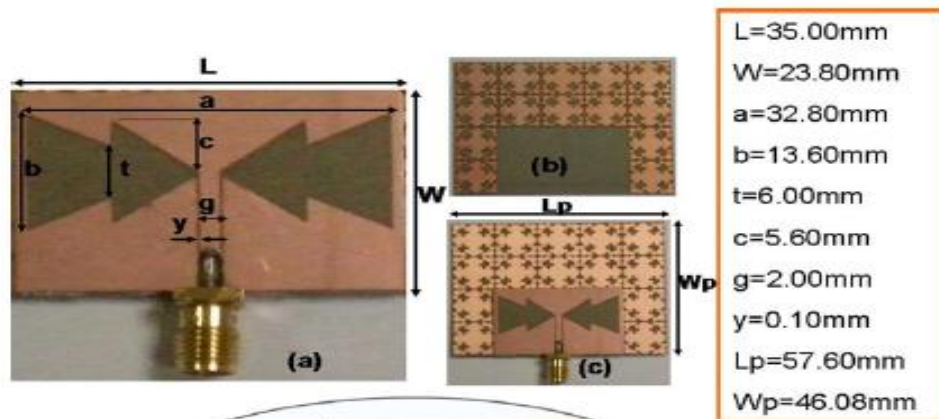


Figure 22: Element of the manufactured prototype ,(a) double bowtie antenna ,(b)AMC unit cells arrangement ,(c) Bowtie AMC prototype .(25)

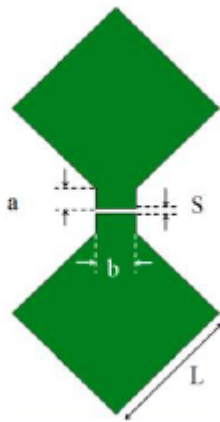
The combined structure Bow-tie–AMC is placed on a metallic plate, the current distribution on the bow-tie is not affected, so it is possible to affirm that the AMC electromagnetically insulates the bow-tie antenna from the metallic plate. The Radiation pattern properties of the Bow-tie–AMC for RFID application are still preserved even when placed on a metallic plate and the gain increased until 9, 23 dB.

In (26) the diamond dipole antenna is printed on a CuClad substrate with thickness $h_{CuClad} = 1.58$ mm, relative permittivity $\epsilon_{CuClad} = 2.5$, and loss tangent $\tan \delta_{CuClad} = 0.0018$ with bandwidth of 53% (4.56-7.84 GHz) which feeding by discrete port. as shown in Figure 23. Due to the stacked nature of the antenna with AMC reflector, it is proposed to feed the antenna with a 50 Ω SMA connector placed at the edge of the antenna substrate, that's why the balun is used.

The AMC is an array of square copper patches printed on a FR4 Epoxy substrate with $\epsilon_{FR4} = 4.0$, $\tan \delta_{FR4} = 0.02$, and a thickness of $h_{FR4} = 3.2$ mm backed by a metallic ground plane and the dimensions of AMC are found out to be $W_{AMC} = 7.4$ mm, $g_{AMC} = 1$ mm. The phase interval of reflection coefficient leading to constructive interference in antenna plane (-90° , $+90^\circ$) is from 4.2 to 5.8 GHz (32%).

The AMC is an array of square copper patches printed on a FR4 Epoxy substrate with $\epsilon_{FR4} = 4.0$, $\tan \delta_{FR4} = 0.02$, and a thickness of $h_{FR4} = 3.2$ mm backed by a metallic ground plane and the dimensions of AMC are found out to be $W_{AMC} = 7.4$ mm, $g_{AMC} = 1$ mm. The phase interval

of reflection coefficient leading to constructive interference in antenna plane (-90° , $+90^\circ$) is from 4.2 to 5.8 GHz (32%).



DIMENSIONS OF THE DIAMOND DIPOLE	
Parameter	Value (in mm)
L	9.0
S	0.3
a	1.5
b	3.0

Figure 23: Diamond dipole antenna.(26)

A split radiation pattern in the broadside direction appearing when using an Artificial Magnetic Conductor (AMC). The reason behind this behavior is perceived to be the presence of surface currents on the AMC that cause destructive interference and lead to loss of gain in broadside radiation pattern at 5.8 GHz. A hybrid reflector(as shown in Figure.24) is then proposed to mitigate this problem by using both electrical and magnetic conductors. This solution enhances the gain. The antenna has a usable bandwidth of approximately 46% (4.2 - 6.7 GHz) and a variation of gain in the whole band between 4.9 and 7.9 dBi.

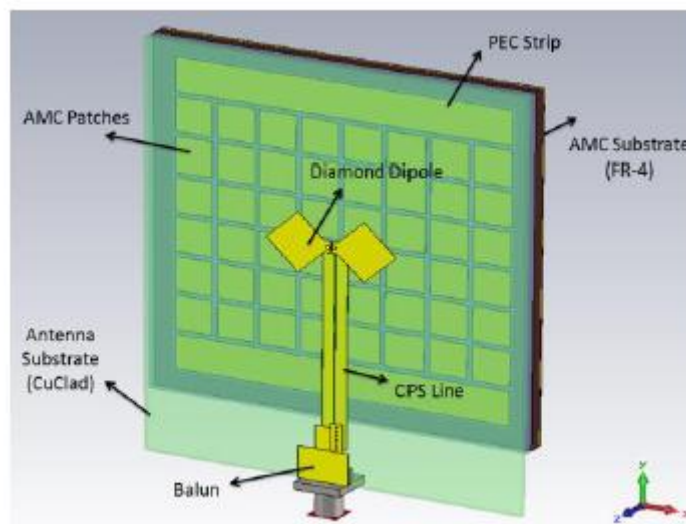


Figure 24: Final antenna with hybrid reflector.

In (27) , a low profile and Broadband slot antenna with an artificial magnetic conductor (AMC) surface is designed for X and Ku communication, fed with the coplanar waveguide (CPW), the designed slot antenna consists of two radiating slot with evolved C-shaped branches.

The proposed structure is designed from the L-slot antenna loaded with C-shaped slot branches and adding two L-shaped branches on the ends of each C-shaped branch.(Figure 25)

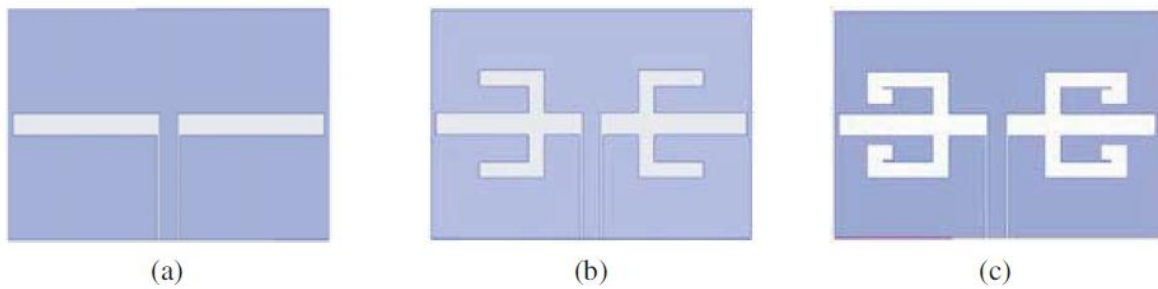


Figure 25: Geometry of the three types of slot antennas. (a) Slot antenna1, (b) Slot antenna2 and (c) the proposed structure.

The AMC unit cell is made up of two central hexagonal with six rectangle branches, operates in a wide in-phase reflection frequency band ranging from 6 to 13.94GHz at the reference plane 4 mm above the AMC surface which is composed of 8×10 AMC unite cells located under the slot antenna with a distance of approximately 0.107λ .(Figure .26).

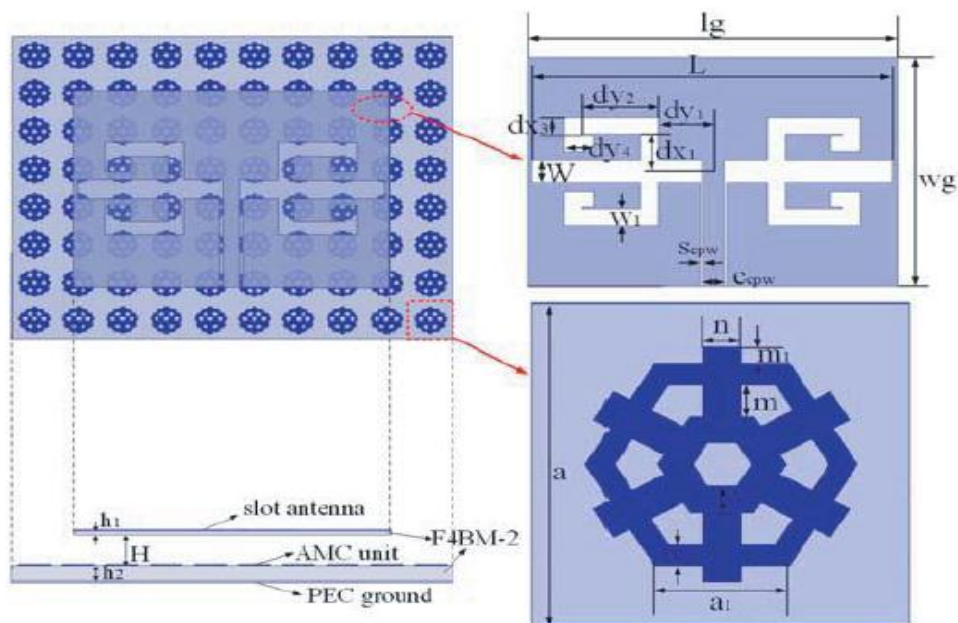


Figure 26: Top and side views of the composite antenna. (27)

The composite antenna achieves a wide impedance bandwidth from 7.64GHz to 14.58 GHz(62.47%). and exhibit a maximum gain of up to 10.26 dBi, high front-to-back ratios and low cross-polarization level, which enable the proposed antenna to be utilized in X and Ku communications.

II.7 Conclusion:

According to the definition and the application of the EBG structures, we have seen the advantages of using artificial magnetic reflector for navigation and communication systems. In fact, we can design antennas with a low profile, and high directivity. In addition, a state of the art on wideband antenna with artificial magnetic reflector has been done.

Chapter III

Wideband bow-tie antenna with an Artificial Magnetic Conductor (AMC)

Chapter III: Wideband bow-tie antenna with an Artificial Magnetic Conductor (AMC).

III.1 Introduction

In this chapter, a planar wideband bowtie antenna is first presented. This antenna is then studied with an artificial magnetic conductor (AMC) to redirect the energy back in half space and increase the gain, with a reduction of thickness antenna. After that, a parametric studies on structure geometry is done with CST Microwave Studio to have a maximum stable gain on the C band.

III.2 CST Microwave Studio Simulator

Microwave-studio software from CST (Computer Simulation Technology) is electromagnetic simulation software with 3-dimensional structure. We use the time method (Transit solver) of the Microwave software. The choice was focused on this software because the use of such a resolution tool in the time domain is suitable for large structures. CST Microwave Studio uses the Finite Integral Technique. The FIT method is a generalization of the Finite Difference Time Domain method. It consists of a spatio-temporal discretization of Maxwell's equations in an integral formulation. The computational domain is broken down into cubic elementary cells.

III.3 Bowtie Antenna

A compact wideband antenna with an integrated balun, which achieves a very large bandwidth (2.5GHz-14 GHz), is presented in. It consists of a printed modified Bow-tie antenna fed by an integrated compact wideband balun illustrated in Figure .27. The overall size of the antenna printed on FR4 substrate is $75 \times 58 \text{ mm}^2$. The antenna achieves a low gain (2.5 dBi) and unstable radiation pattern from 6 GHz. The optimized dimensions of the bow-tie antenna and the balun are as follows: $L_p = 75 \text{ mm}$, $W_s = 58 \text{ mm}$, $L_p = 46 \text{ mm}$, $W_p = 28 \text{ mm}$, $X = 0.3 \text{ mm}$, $W_{add} = 10 \text{ mm}$, $L_{mcs} = L_m = 12 \text{ mm}$, $W_{mcs} = 3.137 \text{ mm}$, $W_m = 20 \text{ mm}$, $L_{cps} = 8.25 \text{ mm}$, $W_{cps} = 0.3 \text{ mm}$, $L_t = L_k = 18 \text{ mm}$, $W_k = 10.15 \text{ mm}$.

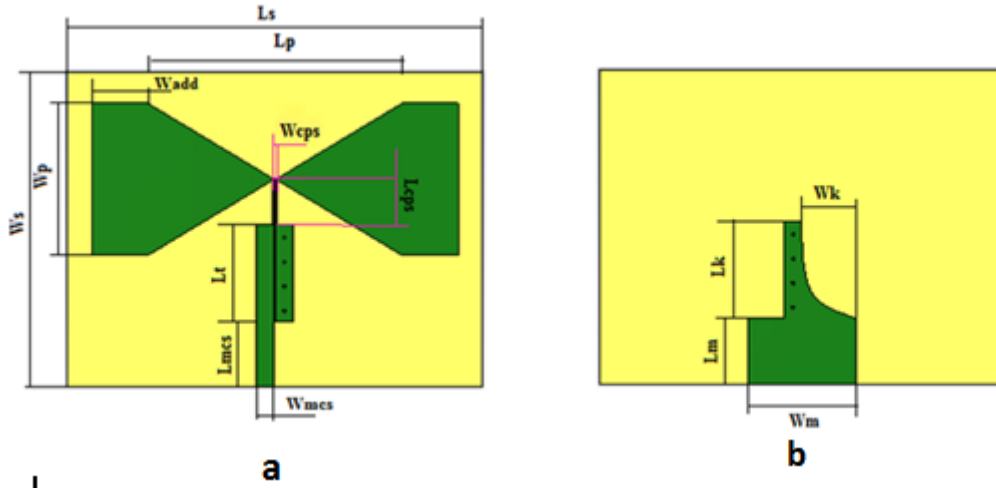


Figure 27: Dimensions of bowtie + balun: (a) Top view and (b) Bottom view(28).

The aim is to provide with this bowtie antenna a better stable radiation patterns in C-band and allow its integration on an satellite with a low thickness and a low weight. For this reason, we propose to put an AMC under the bowtie antenna.

III.4 AMC reflector design

The AMC reflector is composed of metallic square patches etched on a grounded substrate. There is no via between the patch and the ground plane, which enables to reduce the cost and facilitate the realization. The unit cell geometry is presented in Figure 28.

In order to design an AMC whose frequency band is included within the operational band of the Bow-Tie, the following dimensions have been chosen: $L_{amc}=9.4$ mm, $W_{amc}=8$ mm, $g_{amc}=0.7$ mm. The FR4 is used with permittivity $\epsilon_r = 4.3$.

To design the unit cell, the appropriate boundary conditions must be defined to introduce a TEM (plane wave) mode whose direct trihedron is formed by the E and H fields. Only one element of the infinite structure is considered. The orthogonality of the fields is obtained from electrical boundary conditions along an axis on either side of the cell and magnetic boundary conditions along the perpendicular axis. The phase of the reflection coefficient of the structure is then determined only for normal incidence. The CST software makes it possible to specify these boundary conditions as shown in Figure 29.

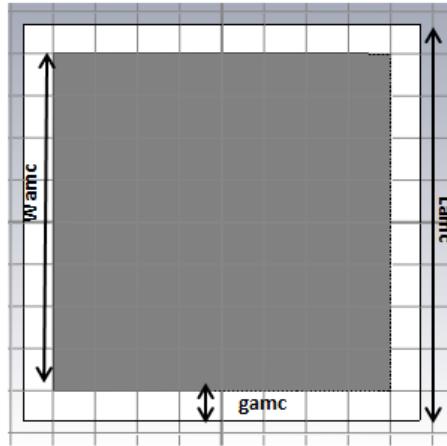


Figure 28: AMC cell.

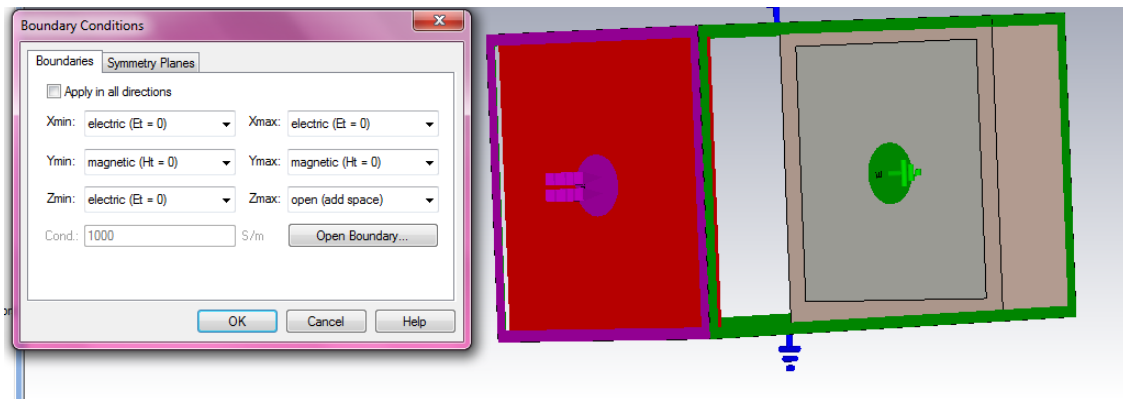


Figure 29: Boundary conditions of the AMC structure.

We put for; **Xmin** and **Xmax**: $E_t = 0$ to have the horizontal electric field as shown in Figure 30.a).

Ymin and **Ymax**: $H_t = 0$ to have the vertical magnetic cage as shown in Figure 30.b.

Once the boundary conditions are established, the structure is placed at a distance $D \geq \frac{2 \times a^2}{\lambda}$ from the source to be in the far field zone, as shown in Figure 31:

- D: distance to the cell in m.
- a: the largest dimension of the antenna expressed in m.
- λ : wavelength in m.

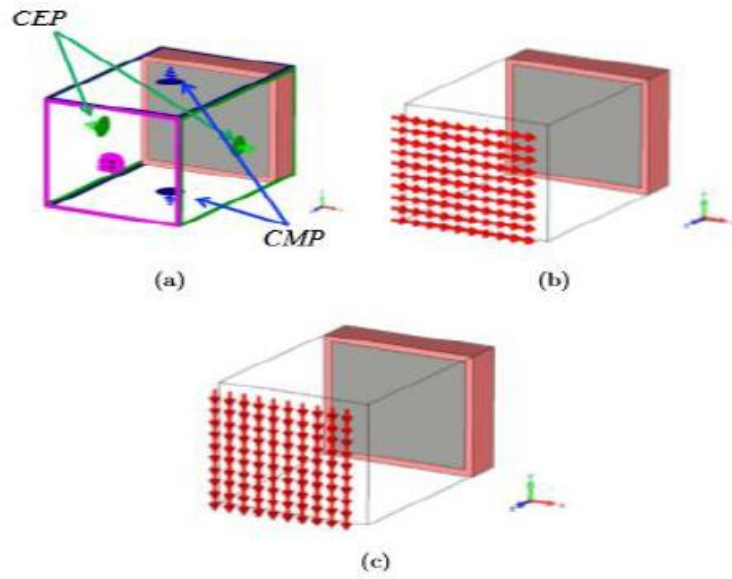


Figure 30: Boundary conditions of a structure.

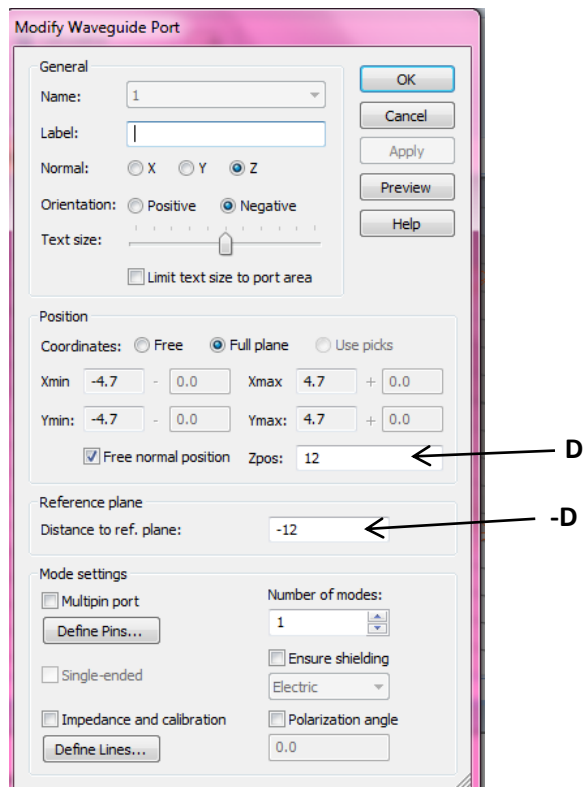


Figure 31: Far filed distance in Wave guide port

After simulation of the AMC cell, we represent the phase diagram in Figure 32. It shows that the high impedance structure has a phase between -90° and 90° in the frequency band 4.23-5.89 GHz with relative bandwidth of 32.8%.

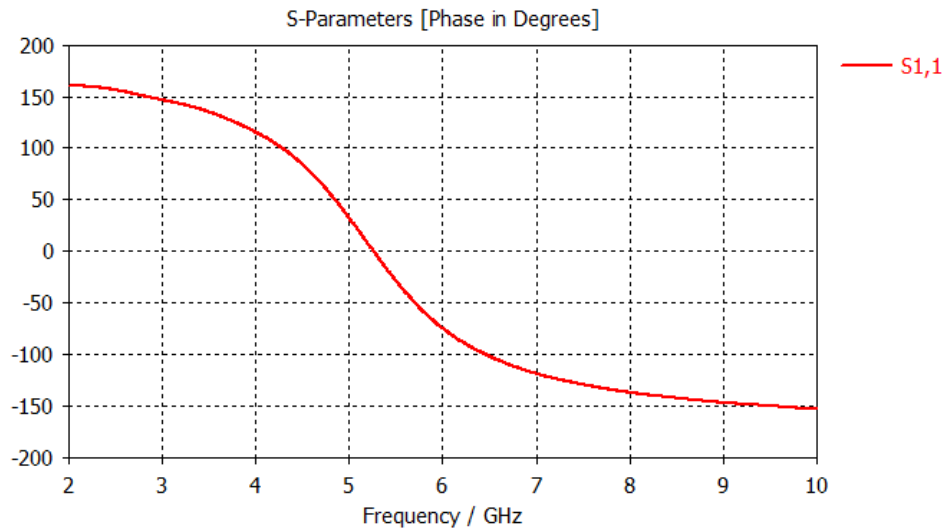


Figure 32: Phase reflection coefficient.

III.5 Bowtie antenna over artificial magnetic conductor

We analyze performance of the antenna when placed over an AMC designed using 8x8 unit cells, as shown in Figure33. For this purpose, simulations are carried out in CST Microwave Studio to see the reflection coefficient and the gain en broad side. The distance between antenna and AMC plane is $h_{air} = 2mm$. H_{air} is chosen so as keeping the most possible frequency bandwidth matched in the operating frequency band, as well as maintaining constructive interference in broadside direction. The overall thickness of the radiating structure becomes 6.8 mm.

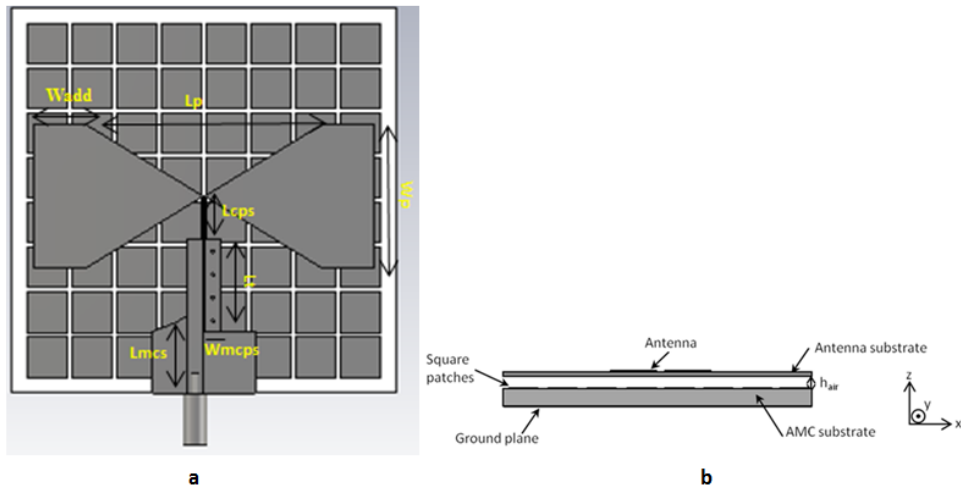


Figure 33: Bowtie antenna over AMC with 8*8 cells: (a) Front view, (b) side view.

The whole structure is simulated with 8*8 cells. Results in terms of reflection coefficient are presented in Figure 34. It observed a antenna mismatching, in particular at low frequency (between 3 and 4 GHz), and around 8 GHz because the reflection coefficient is upper then -10 dB. In addition, the gain in broadside direction still low and not stable in the whole bandwidth, as can be deduced from Figure 35.

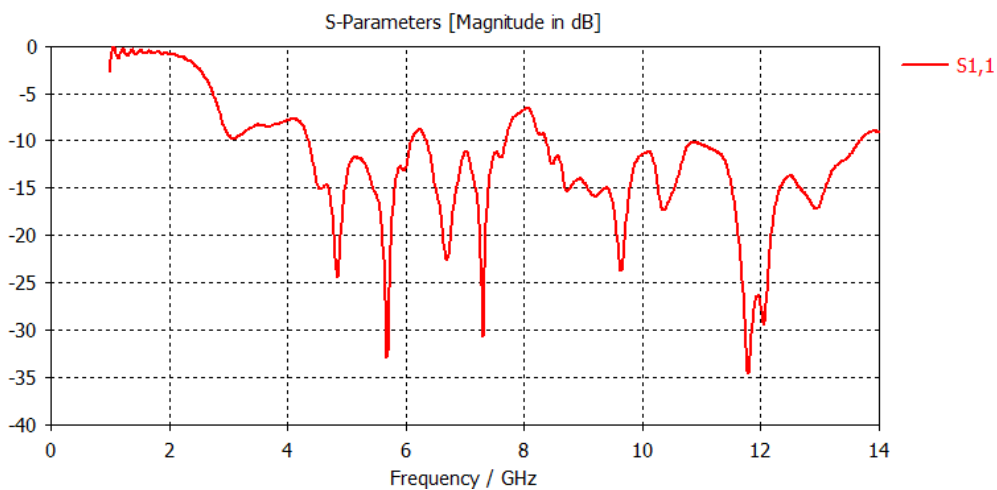


Figure 34: Reflection Coefficient S_{1,1}.

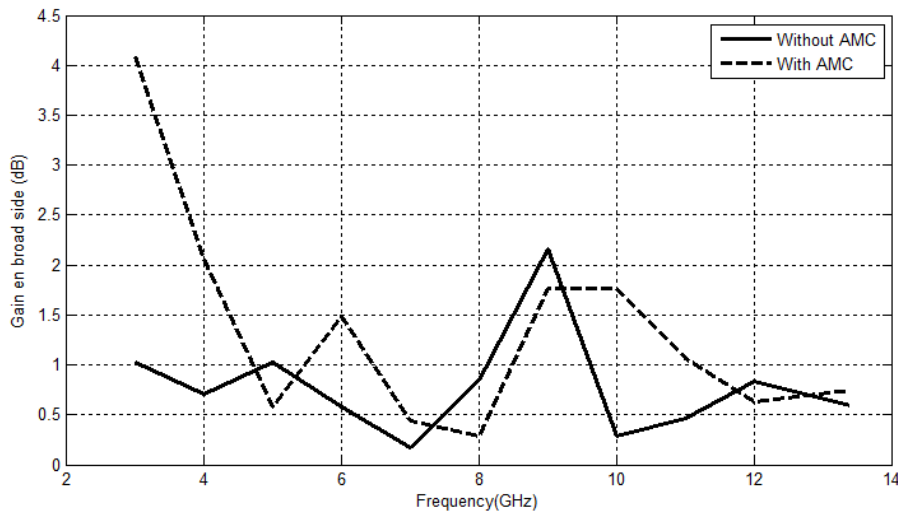


Figure 35: Broadside realized gain of 8x8 AMC-based antenna and without AMC.

The behavior of the whole structure (bowtie+AMC) is studied by analyzing its surface current. In fact, it is well known that a surface on which a uniform current is circulating exhibits a directive radiation pattern with a main beam in the direction normal to the surface (broadside direction). Furthermore, the larger the surface, the greater the directivity. However, when the surface becomes large compare to the wavelength, the current distribution may be not uniform and the current phase may range between 0° and 360° thereby inducing some opposite phase current (26). Consequently, destructive interference may occur a degradation gain. This effect is particularly undesirable. To understand if this effect happens, the surface current of the 8x8 AMC-based antenna designed is observed in Figure 36. The current is mainly concentrated and spread over AMC which led to destructive interference and low gain. In addition, putting AMC cells behind the balun disturb significantly the distribution of current. For this reason, we removed AMC cells that are close to balun as shown in Figure37.

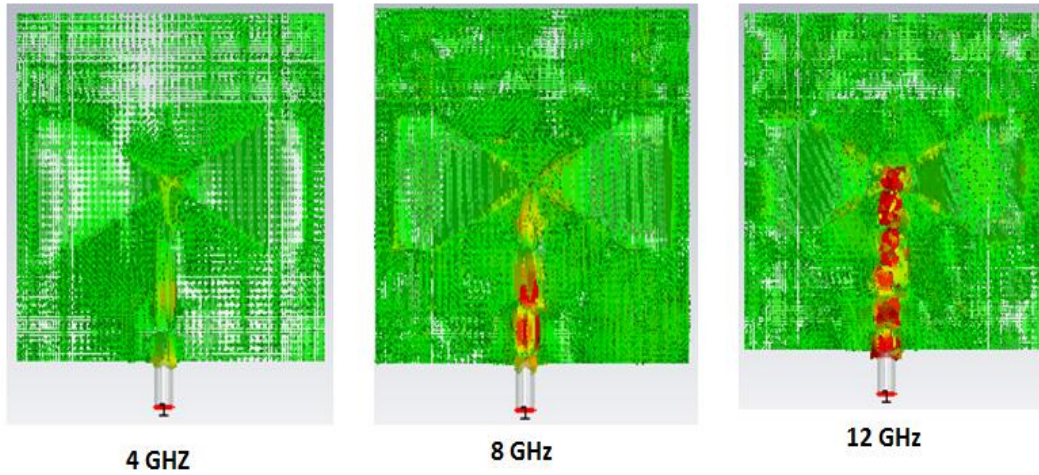


Figure 36 current distribution in AMC 8x8 at: 4 GHz, 8GHz and 12 GHz.

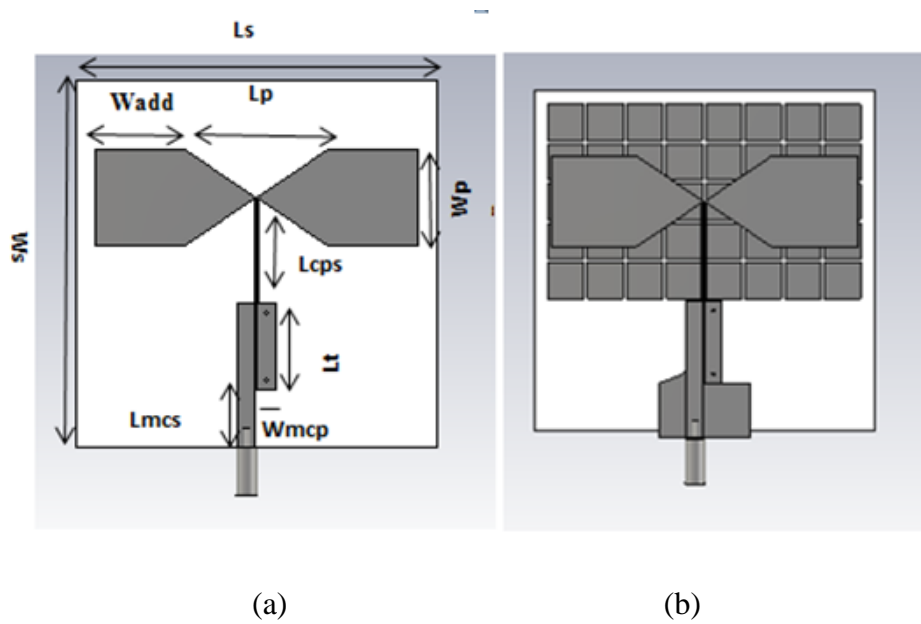


Figure 37: Dimensions of the overall structure (bowtie + balloon at AMC with 8*5 cells): (a) Top view and (b) Bottom view.

III.6 Parametric study

Antenna structure dimensions affect significantly its performances. A parametric study is done in order to have a reflection coefficient less than -10 dB on the widest possible band (around the C band) with a stable gain.

III.6.1 Influence of the parameter L_{cps}

In this part, we will study the influence of the variation of the length L_{cps} , on the reflection coefficient and the realized gain in broad side of the antenna as presented in Figure 38 and Figure 39. The length L_{cps} is varied from 16 mm to 22 mm.

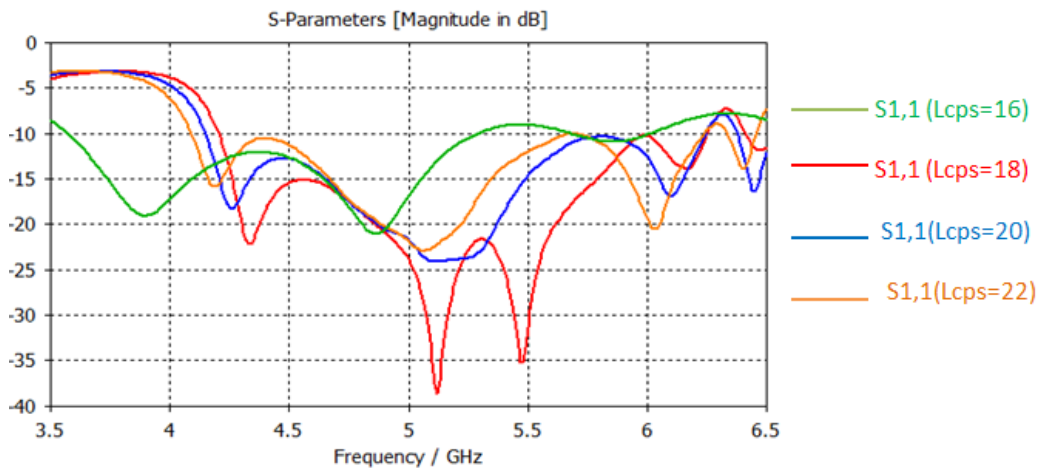


Figure 38: Reflection coefficient of the variation of the parameter L_{cps}

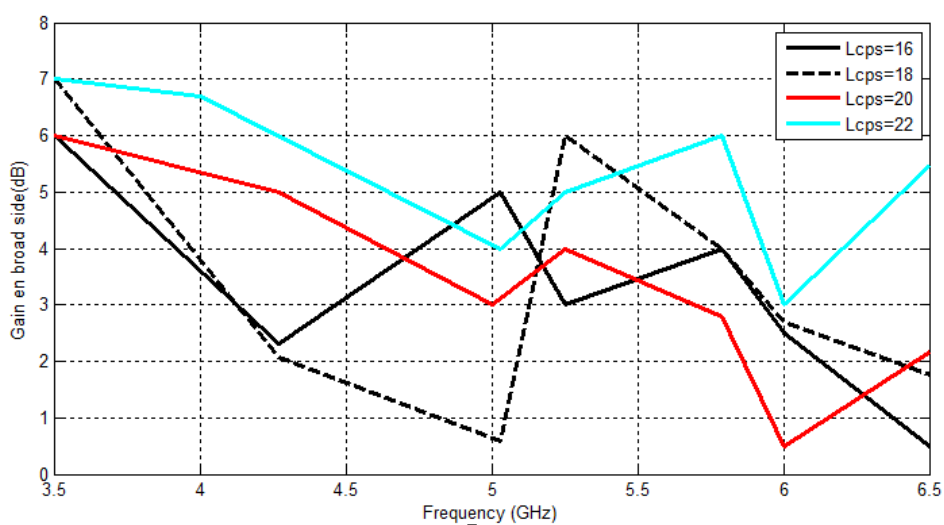


Figure 39: Gain en broad side of the variation of the parameter L_{cps} .

These results show that reflection coefficient is less than -10 dB in the C-band for the values 18, 20, and 22 mm. Regarding the realized gain in broadside direction, we observe that we have the best results for whole band for $L_{cp}=22$ mm. Therefore we will keep this value for the rest of study.

III.6.2 Influence of the parameter L_p

In this part, we will study the influence of the variation of the length L_p , on the performance of the antenna, presented in Figure 40 and Figure .41. The length L_p is varied from 15mm to 30 mm. This results show that the reflection coefficient is less than -10 dB in the C-band for all L_p values. In the other hand, when L_p decreases the realized gain in broadside direction is decreased. Therefore, we will chose $L_p=30$ mm because it present the maximum gain (between 5.5 and 7.1 dBi in the band 4 to 5.75 GHz).

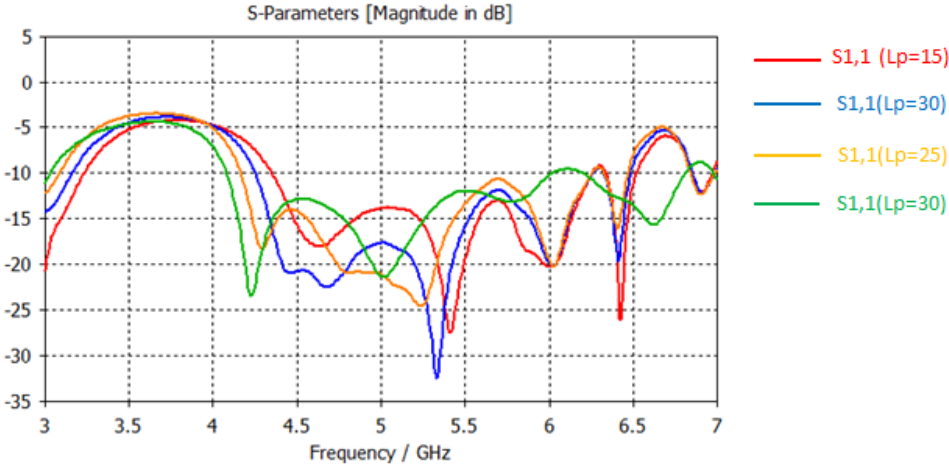


Figure 40: Reflection coefficient of the variation of parameter L_p .

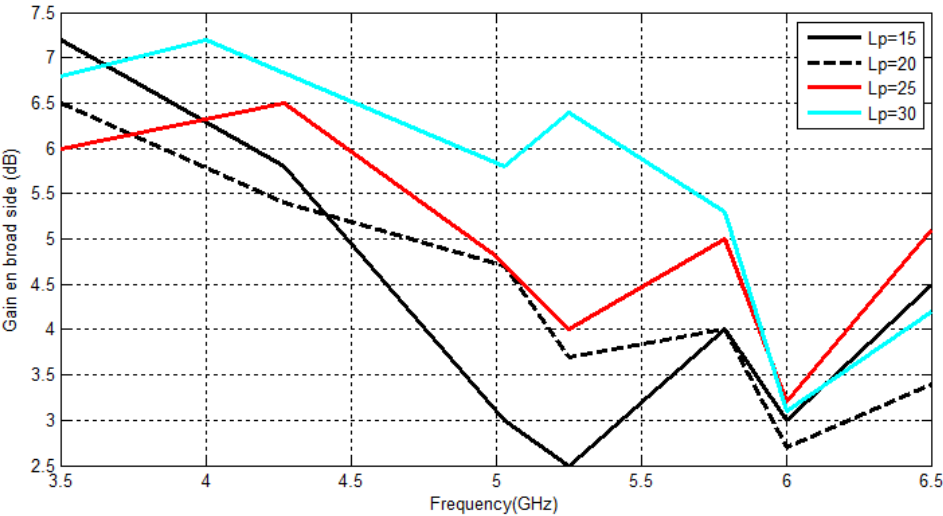


Figure 41: Gain in broad side of the variation of parameter L_p

III.6.3 Influence of the parameter W_p

We will present the influence of the variation of the length W_p on the performance of the antenna, presented in Figure 42 and Figure 43. The length W_p is varied from 15.13mm to 30.13mm. These results show that reflection coefficient is less than -10 dB in the C-band for the only values 15.13 and 20.13. Regarding the realized gain in broadside direction, we observe that we have the best results for whole band for $L_{cps}=20.13$ mm. Therefore we will keep this value for the rest of study.

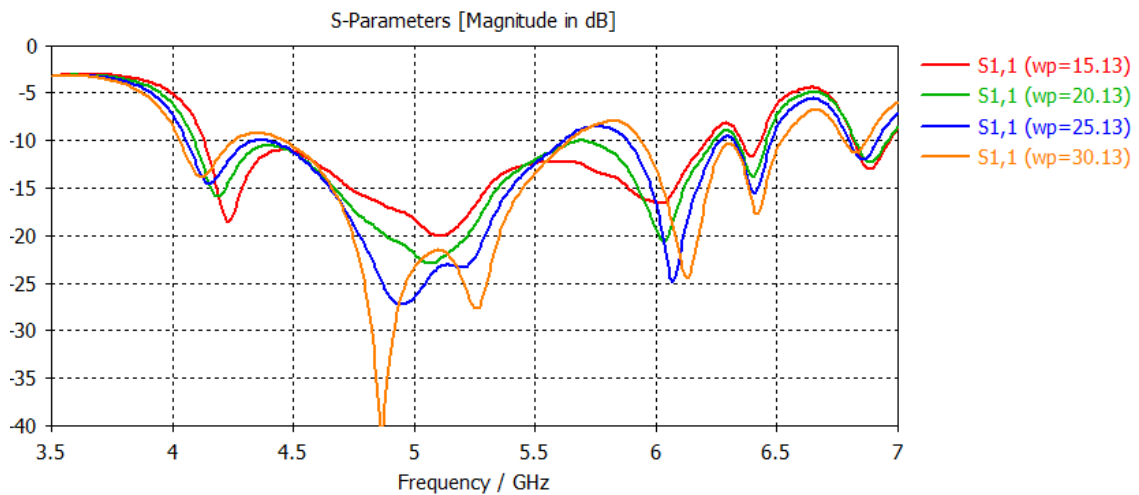


Figure 42: Reflection coefficient of the variation of parameter W_p .

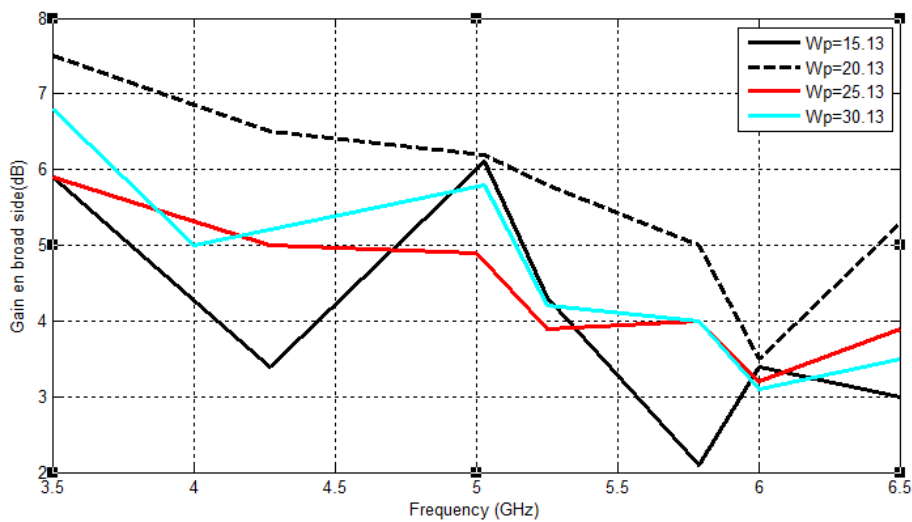


Figure 43: Gain in broad side of the variation of parameter W_p .

III.6.4 Influence of the parameter Wadd

Now, we will focus on the influence of the variation of the parameter Wadd on the reflection coefficient and the realized gain in broadside. The length Wadd is varied from 6.66 mm to 24.66 mm, as shown in Figure 44 and Figure 45 . The result shows that all the values of Wadd allow a good marching in the C-band, but the best gain is obtained for when Wadd=18.66mm. Therefore we will keep this value for the rest of study.

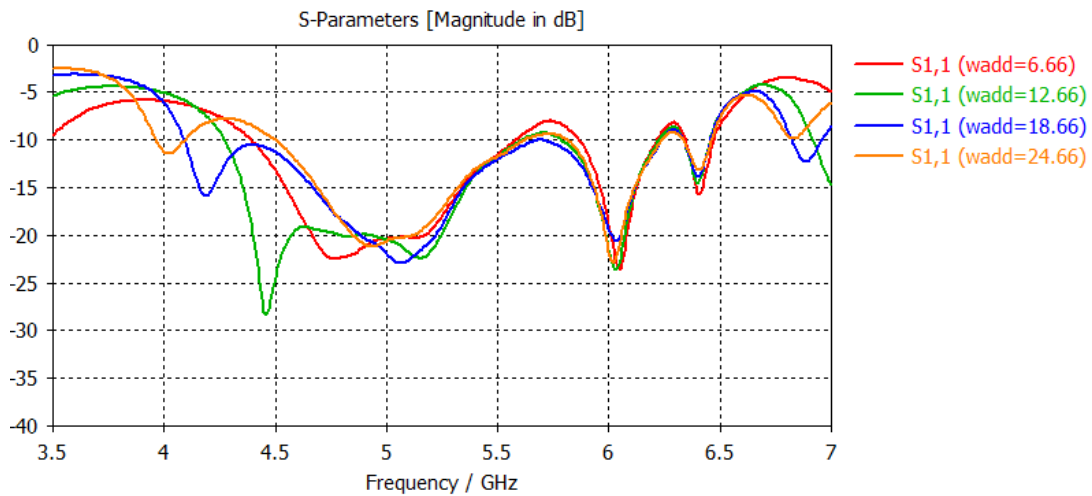


Figure 44: Reflection coefficient of the variation of parameter Wadd.

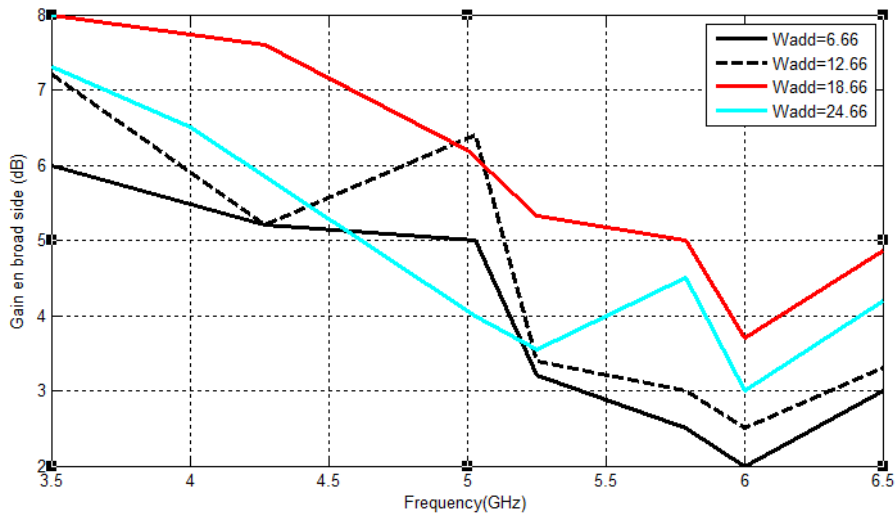


Figure 45: Gain in broad side of the variation of parameter Wadd.

III.6.5 Influence of number of vias

In this section we see reflection coefficient and the realized gain in broadside for different number of vias (2, 3, 4 vias), as shown in Figure 46 and Figure 47. As we can see, there is no significant difference on the impedance matching but a significant enhancement is observed in the realized gain in broadside when we use two vias .

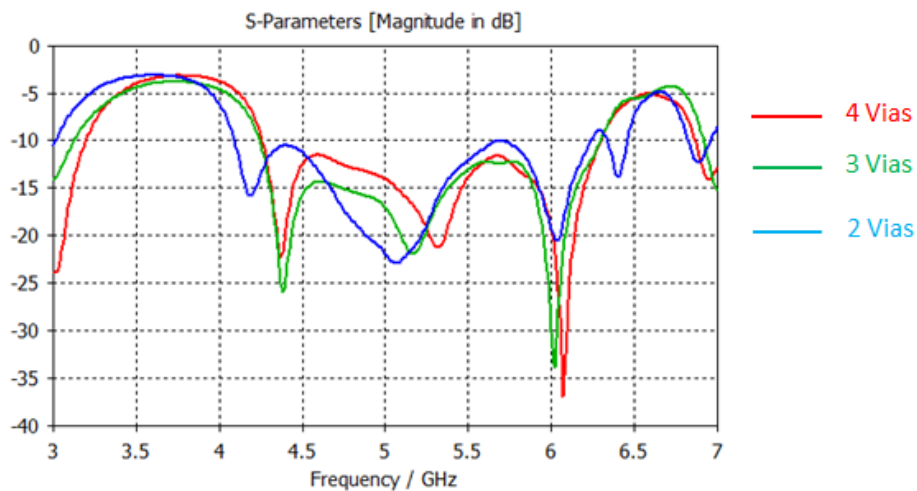


Figure 46 : Reflection coefficient of the variation of vias number.

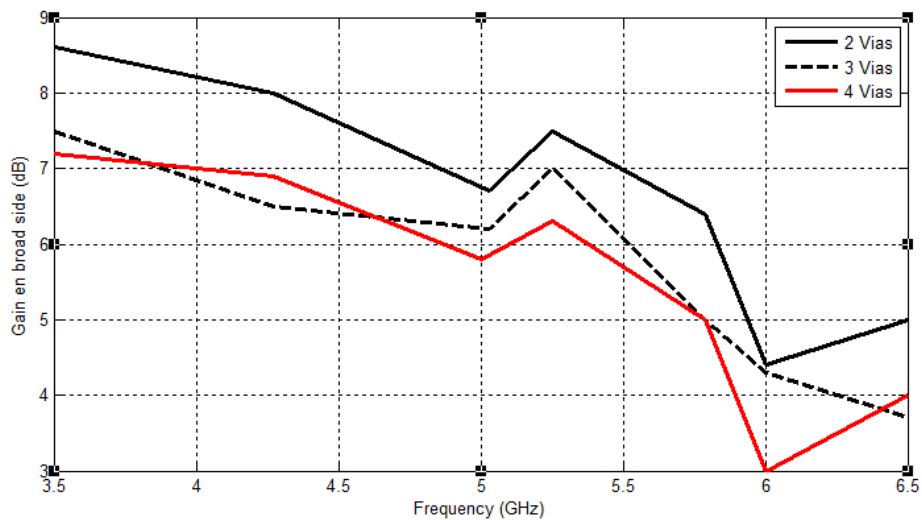


Figure 47: Gain in broad side of the variation of vias number.

III.7 Optimized structure

After the parametric study and optimization, we have obtained the optimal structure. The optimized dimensions of the bow-tie antenna over a AMC with 5*8 cells are as follows: $L_s=75$ mm, $W_s =76.5$ mm, $gap =0.3$ mm , $L_p=25$ mm , $W_p=20.13$ mm , $L_{cps}=18$ mm , $L_t=18$ mm , $W_{cps}=0.3$ mm $L_{mcs}= 12$ mm , $W_{add}=18.66$ mm, $W_{mcps}=4$ mm. Figure.48 shows the simulated magnitude of reflection coefficient performances of the antenna. As seen the simulated bandwidth of this antenna is 2.32 GHz (4.08-6.4 GHz).

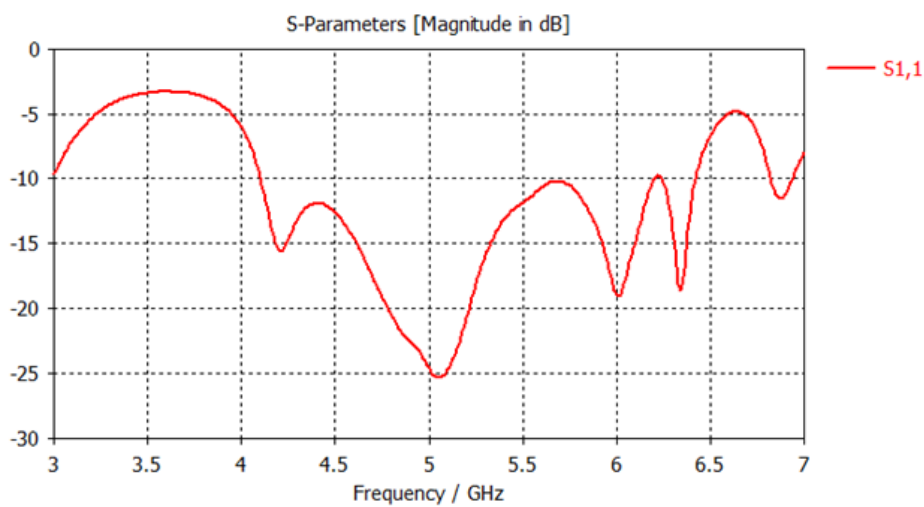


Figure 48: Reflection coefficient of the optimized structure.

In the other hand, a significant improvement is observed in the realized gain of the whole band, as shown in Figure.49. In fact, the comparison of the antenna with and without AMC shows that the gain in broadside increases significantly over the whole band. An improvement of 8 dBi in broadside gain is observed at 4.08 GHz. Maximum gain in the bandwidth is $G_{max} = 8.8$ dB at 4.08 GHz. This is primarily due to the high current concentration on the balun and the bowtie as shown in Figure.50. At 6 GHz, a minimum is observed in the radiation pattern with 4.3 dBi. However, for frequency 6 GHz, the currents are more spread out over the structure leading to the low gain (4.3dBi) as shown in Figure.51. Figure.52 shows the directive radiations patterns of the optimized structure at different frequencies (4.08 GHz, 4.7 GHz, 5.28 GHz, 5.8 GHz and 6.4 GHz.).

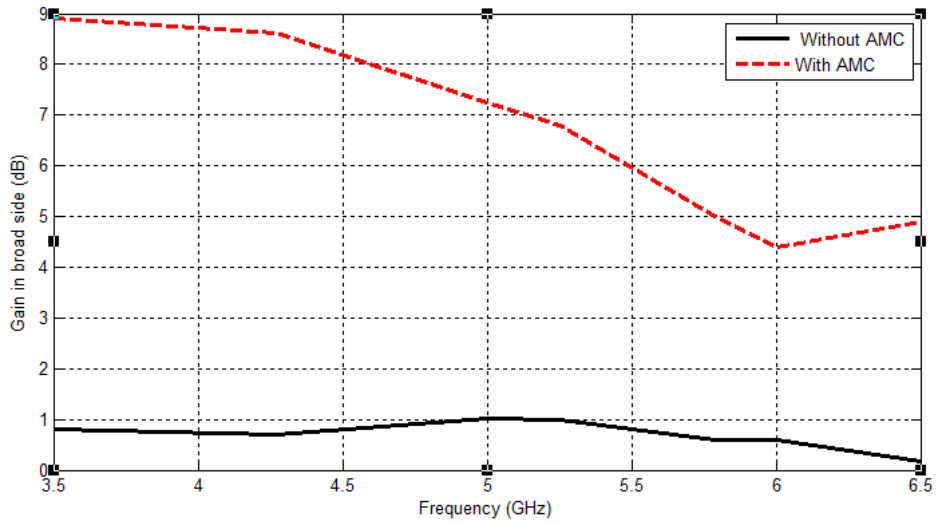


Figure 49: Realized gain vs. frequency in the broadside direction.

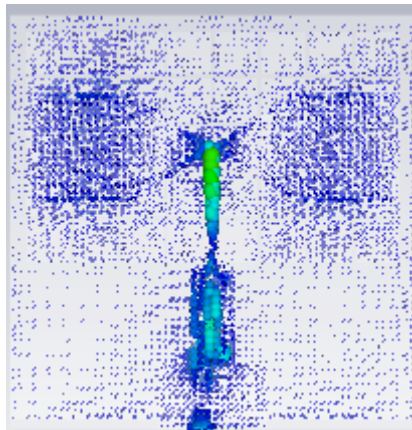


Figure 50 : Current distribution at 4 GHz.

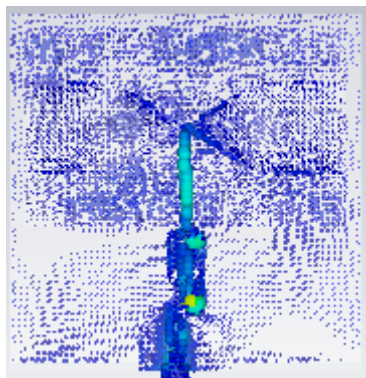


Figure 51: Current distribution at 6 GHz.

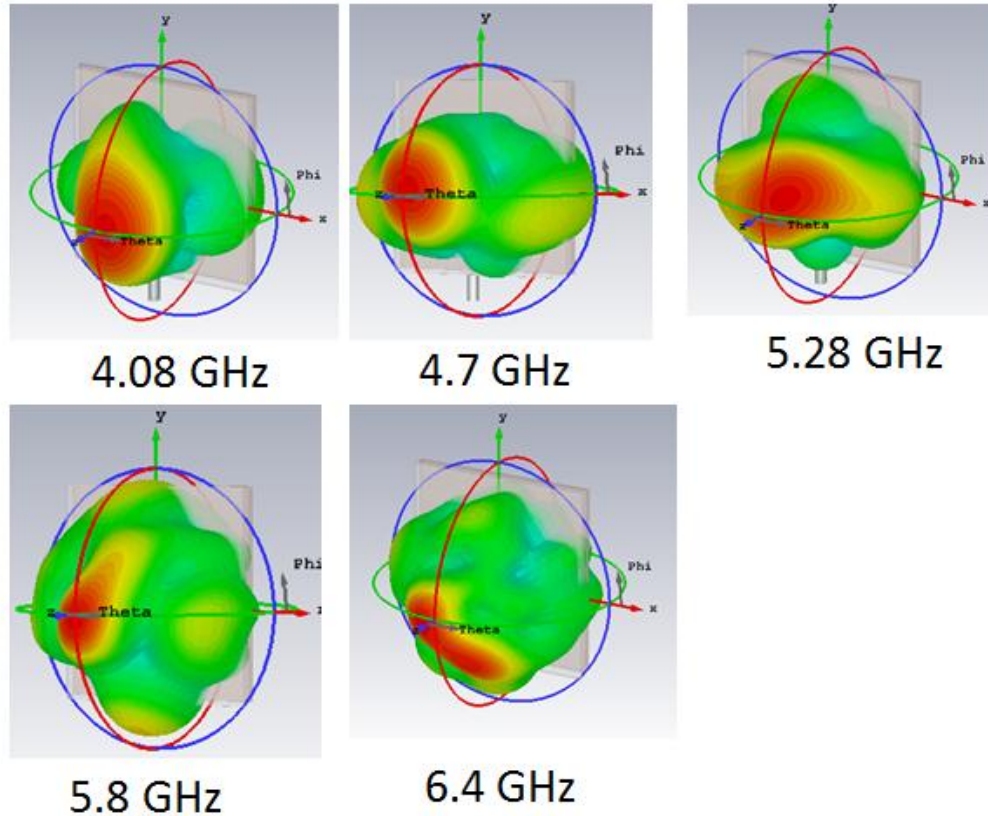


Figure 52: The directive radiations patterns of the optimized structure at 4.08 GHz, 4.7 GHz, 5.28 GHz, 5.8 GHz and 6.4GHz.

III.8 Conclusion

In this manuscript, Artificial Magnetic Conductor (AMC) reflector is used to improve wideband antennas' performances. AMC is inherently narrow band. However, it has been shown that the bandwidth of AMC-based antennas can exceed the AMC bandwidth alone in terms of impedance matching. Nevertheless, some issues regarding the radiation pattern are reported. In particular, maintaining a high gain value toward a given direction over a wide frequency range is a difficult task. Designing the antenna and the AMC separately does not lead to optimal performances and that adjustment in designs is necessary and done with parametric study. The proposed structure is a compact wideband bowtie antenna with AMC reflector. Besides, its low thickness ($\lambda/10$ at the center frequency of operation, i.e. 5.24 GHz), this structure is very simple and low cost. This antenna operates over wide band, is from 4.08 to 6.4 GHz (C band) which suitable for spatial applications. Its radiation patterns are directive and vary from 4.3 dBi to 8.8 dBi.

Conclusion and perspectives

The work presented in this manuscript is the design of an antenna with low-profile, high-gain and wide bandwidth for C-band applications such as radar applications and satellite communications. To do this, we first presented the satellite navigation system as well as the satellite communication system. Then we present the different antenna types used in the two space systems. So more applications have frequency deferent required more antennas. In addition, we saw that each application required a specific frequency which needs to have several antennas on the same airborne. Consequently, we propose to use a wideband antenna in order to, avoid using several antennas. In the other hand, an antenna embedded on satelliteneeds to radiate outside the satellite, while preventing the electromagnetic contamination of its internal environment.

According to the EBG definitions and applications, we found that AMC reflector is a good solution to achieve our purpose. A compact wideband bowtie antenna over an AMC reflector of with $5 * 8$ cells with dimensions of $75 \times 76 \times 3.2$ mm³, operating in the C-band, is proposed .Besides, its low thickness ($\lambda/10$ at the center frequency of operation, i.e. 5.24 GHz), this structure is very simple and low cost. This antenna operates over wide band, is from 4.08 to 6.4 GHz which is suitable for spatial applications. Its radiation patterns are directive and vary from 4.3 dBi to 8.8 dBi in the whole band. Thanks to AMC reflector, an improvement of 8 dBi in broadside gain is achieved.

The perspective of this work is to realize the proposed structure, measured it and validates the simulation results.

References

1. **Jhon Walker, Joseph L Awange.***Surveying for Civil and Mine Engineers.* Australia : Springer, 2017.
2. **Richard B. Langley, Peter J.G. Teunissen, Oliver Montenbruck.** *Introduction to GNSS, 2017.*
3. **K. Czaplewski, D. Goward.** 2016 *Global Navigation Satellite Systems – Perspectives on Development and Threats to System Operation.*
4. **Jing Li, Jiantong Zhang, Bingqi Zhang, Bing Shen ,** *Operation and Development of BeiDou Navigation Satellite System..* Beijing, China : s.n., October 2015. 978-1-4673-7634-1/15.
5. **Awange JL (Awange JL (2012) Environmental monitoring using GNSS. Springer, Heidelberg,) Environmental monitoring using GNSS. Springer, Heidelberg,.Envirement monitoring using GNSS.** Springer, Heidelberg, NEW York : s.n., 2012 .
6. **Matin, M. A.***Communication Systems for Electrical Engineers.* s.l. : springer. ISBN 3319701282.2018.
7. **G. Maral, M. Bousquet, Z. Sun.***Satellite Communication Systems: Systems, Techniques and Technology.* ISBN: 978-0-470-71458-4, December 2009.
8. *Various Types of Antenna with Respect to their Applications: A Review.* **Abdul Qadir Khan, Muhammad Riaz and Anas Bilal.** Islamabad : s.n.,. ISSN: 2045-7057. March 2016.
9. **Tripathi, Dr. V.S.***Micro strip Patch Antenna and its Applications: a Survey.* ISSN:2229-6093, 2011.
10. **Gong, M. Karlsson and S.**“An integrated spiral antenna system for UWB.”. October 2015.
11. **A. Agnihotri, A. Prabhu and D. Mishra.***Improvement in Radiation Pattern Of Yagi-Uda Antenna.”.* 2013.
12. **Shashikant Patil, Chinmaya Vyas ,Amar Khalore ,***Spiral Antennas for Communication Engineering Applications: A Systematic Approach..* 2016 : s.n. ISSN 2349-4042 (Print) & ISSN 2349-4050 (Online).
13. **Fateme Ghayem, Farshad Rassaei,***Helical Antenna to Measure Radiated Power Density Around a BTS: Design and Implementation .* China : s.n., 2014.
14. **Bhattacharyya, Arun K ,***Phased Array antenna for Space Applications and Challenges..* December 2017.
15. **William A. Imbriale, Steven (Shichang) Gao and Luigi Boccia.***Space Antenna Handbook.* 2012.
16. **Nacer Chahat, Richard Hodges, Jonathan Sauder, Eva Peral, Yahya Rahmat-Samii.***CubeSat Deployable Ka-band Mesh Reflector Antenna Development for Earth Science Missions.*
17. **Fan Yand, Yahya Rahmat-Samii.***Electromagnetic Band Gap Structures in Antenna Engineering.* ISBN-13 978-0-511-45579-7, 2008.
18. **NADER ENGHETA, RICHARD W. ZIOLKOWSKI.***METAMATERIALS Physics and Engineering Explorations,* ISBN-13 978-0-471-76102-0, 2006.

19. **Dan Sievenpiper, Lijun Zhang, Romulo F. Jimenez Broas, Nicholas G. Alexopolous, Eli Yablonovitch** ,*High-Impedance Electromagnetic Surfaces with a Forbidden Frequency Band.* . s.l. : IEEE TRANSACTIONS ON MICROWAVE THEORY AND TECHNIQUES, NOVEMBER 1999.
20. **A. Dellavilla, V. Galdi, F. Capolino, V. Pierro, S. Enoch, and G. Tayeb.***A Comparative Study of Representative Categories of EBG Dielectric Quasi-Crystals.* s.l. : IEEE Antennas Wireless Propagat. Lett, vol. 5, 331–4,, 2006.
21. **Wang, C. Gao and Y.***Analysis of EBG structures implemented on CPW components by using EM-ANN models .* June 2002.
22. **K. Brakora, C. Barth, and K. Sarabandi,***plane-wave expansion method for analyzing propagation in 3D periodic ceramic structures.* july 2005.
23. **Yong-Wei Zhong, Guo-Min Yang and Li-Rong Zhong** ,*Gain enhancement of bow-tie antenna using fractal wideband artificial magnetic conductor ground.* February 2015.
24. *A Novel Low-Profile High-Gain Antenna Based on Artificial Magnetic Conductor for LTE Applications.* **Fen-hua Yang, Wei Tang.** Fujian, China : s.n., 2012.
25. **Hadarig, María Elena de Cos Gomez, Y. Álvarez and F. Las-Heras,***Novel Bow-tie–AMC Combination for 5.8-GHz RFID Tags Usable With Metallic Objects.* IEEE ANTENNAS AND WIRELESS PROPAGATION LETTERS, 2010.
26. **Chetan Joshi, Anne Claire Lepage, Julien Sarrazin and Xavier Begaud***Enhanced Broadside Gain of an Ultra-Wide Band Diamond Dipole Antenna using a Hybrid Reflector.* 2016.
27. **Xue Yan Song, Tian Ling Zhang, and Ze Hong Yan.***Broadband and Low-Profile Slot Antenna with AMC Surface for X/Ku Applications.* China : s.n., August 2018.
28. **Ouassim, Mr Hadj Youcef and Selloum.***Conception et realisation d'une antenne large bande à balun intégré.* Blida : s.n., 2018.
29. **Wang, H***Antennas for Global Navigation Satellite System (GNSS).* . s.l. : IEEE, July 2012.
30. **Ratni, Badr Eddine.***Étude et conception d'antennes à base de métasurfaces destinées aux applications spatiales et aéronautiques.* paris : s.n., septembre 2017.
31. **P. Ujwala, M. Namrata, K. Pooja, M. Shraddha** "Performance Analysis of corner reflector antenna," *In international journal of innovative research in computer and communication Engineering.* pp. 201-205, 2014.
32. **Balanis, C. A** ,*Antenna Theory Analysis & Design.* "John Wiley, & Sons INC, Third Edition.
33. **Ariel Epstein, Joseph P.S. Wong & George V. Eleftheriades***Cavity-excited Huygens' metasurface antennas for near-unity aperture illumination efficiency from arbitrarily large apertures.* . Toronto, Ontario, Canada : DOI: 10.1038/ncomms10360, Jan 2016.

34. **Yun Bo Li, Lian Lin Li, Bai BingXu, WeiWu, RuiYuanWu, XiangWan, Qiang Cheng & Tie JunCui** *Transmission-Type 2-Bit Programmable Metasurface for Single-Sensor and Single-Frequency Microwave Imaging.* DOI: 10.1038/srep23731, March 2016.
35. **Zhi Hao Jiang, Micah D. Gregory, Douglas H. Werner** *Broadband High Directivity Multibeam Emission Through Transformation Optics-Enabled Metamaterial Lenses.* NOVEMBER 2012.
36. **Nasim Mohammadi Estakhri, Andrea Alù** , *Ultra-Thin Unidirectional Carpet Cloak and Wavefront Reconstruction With Graded Metasurfaces.* s.l. : IEEE ANTENNAS AND WIRELESS PROPAGATION LETTERS, 10.1109/LAWP.2014.2371894, 2014.
37. **He-XiuXu, Shulin Sun, ShiweiTang, Shaojie Ma, Qiong He, Guang-MingWang, TongCai, Hai-Peng Li & Lei Zhou,** *Dynamical control on helicity of electromagnetic waves by tunable metasurfaces.* 2016. | DOI: 10.1038/srep27503.
38. **Karim Achouri, Guillaume Lavigne, Mohamed A. Salem, and Christophe Caloz,** *Fellow Metasurface Spatial Processor for Electromagnetic Remote Control.* s.l. : IEEE TRANSACTIONS ON ANTENNAS AND PROPAGATION, DOI 10.1109/TAP.2537369, 2016.
39. **Sajjad Taravati, Bakhtiar A. Khan, Shulabh Gupta, Member, IEEE, Karim Achouri, and Christophe Caloz** *Nonreciprocal Nongyrotropic Magnetless Metasurface.* IEEE Transactions on Antennas and Propagation . information: DOI 10.1109/TAP.2017.2702712, 2017.
40. **Martin Coulombe, Sadegh Farzaneh Koodiani, and Christophe Caloz** *Compact Elongated Mushroom (EM)-EBG Structure for Enhancement of Patch Antenna Array Performances.* s.l. : IEEE TRANSACTIONS ON ANTENNAS AND PROPAGATION, 10.1109/TAP.2010.2041152, April 2010.
41. **S. John.** *Strong localization of photons in certain disordered dielectric super lattices.* Phys.Rev. Lett., vol. 58, 2486–9, 1987.

